Thesis for the degree of Doctor of Philosophy

Material characterisation for crash modelling of composites

Thomas Bru

Department of Industrial and Materials Science
CHALMERS UNIVERSITY OF TECHNOLOGY
Gothenburg, Sweden 2018

Material characterisation for crash modelling of composites

Thomas Bru

ISBN 978-91-7597-805-5

Doctoral thesis at Chalmers University of Technology

New serial no: 4486

ISSN 0346-718X

Department of Industrial and Materials Science

Chalmers University of Technology

SE–412 96 Gothenburg, Sweden

Telephone + 46 (0) 31 – 772 1000

Cover:
Left side (top left to bottom right); strain map in Iosipescu shear specimen, crushing of 90° coupon, crushing of 0° coupon, micrograph of a ±45° crush coupon.
Right side (top to bottom); damage map in 45° crush coupon simulation, frontal car crash (courtesy of Johan Jergeus at Volvo Cars).

Printed by Chalmers Reproservice

Gothenburg, Sweden 2018

Preface

The work presented in this thesis has been carried out at Swerea SICOMP AB, Mölndal, and at the department of Industrial and Materials Science at Chalmers University of Technology, Gothenburg, during the period October 2013 to September 2018.

This work has been performed within the research projects "Reliable crash modelling of fibre composites for lightweight vehicles – compcrash1/2", with funding from the Swedish Energy Agency through project 34181-1/2. The financial support through these projects is gratefully acknowledged.

My superisor, Robin Olsson, has taught me a lot about mechanics of composite materials. I have tried to question his ideas, but I must admit that Robin is ~~always~~ often right. I have also had the chance to question my own ideas and the freedom to do what I think was important for my research. For this I am very grateful. The support and guidance from my co-supervisor Gaurav Vyas has been invaluable. I also want to thank Professor Leif Asp – Chalmers, for stepping in as co-supervisor at the beginning of last year. In reality, Leif has been involved since the beginning and I have benefited a lot from his impressive range of knowledge about composite materials in general.

My colleagues at Swerea SICOMP, present and former, are acknowelged for their help and for the great time we have had together. Special thanks go to Sérgio Costa for the countless discussions that we have had about our research, Renaud Guktin for contributing with suggestions and comments for the past five years, Spyros Tsampas for his help and advice on fractographic investigations, and Peter Hellström for his assistance in the lab. I also want to thank all the members of the composite research group at Chalmers for the helpful discussions.

Finally I would like to express my sincere thanks to my family, my girlfriend Josefin, and my friends in Gothenburg for their support and encouragement.

Thomas Bru

Gothenburg, September 2018

Abstract

The transport industry must find solutions to reduce its impact on climate change. A promising way to reduce the weight of vehicles and therefore to reduce the CO_2 emissions is to introduce components made of lightweight composite materials, in particular carbon fibre reinforced plastics (CFRPs). Aside from the new design possibilities for lighter vehicle structures, CFRPs can also potentially offer improvements in terms of crash performance in comparison to traditional metallic structures.

During crushing of composite structures, energy is absorbed through the stable progressive failure of the structure. The crushing process is a complex phenomenon involving the interaction of different competing failure mechanisms and frictional interactions taking place at different scales in the material. Today there is no reliable numerical tool to predict the behaviour of composite structures in crash scenarios, which is a hindrance to the introduction of composite materials in mass-produced vehicles. Joint research efforts from both numerical and experimental perspectives are needed to fill this gap.

In this doctoral thesis experiments are carried out to extract relevant material properties for crash modelling, and to assist in the development and the validation of numerical models as a first step of a building block approach with increasing structural complexity. The material selected for the study is a carbon fibre/epoxy uni-weave non-crimp fabric (NCF) composite. The first step in the material characterisation is to extract the different strengths and stiffnesses of the material, which requires dedicated tests because of the orthotropic nature of NCFs. Because several compressive failure mechanisms are driven by the shearing of the matrix polymer, a methodology is presented to extract the damage evolution laws from Iosipescu shear tests and indirect shear tests (uniaxial and biaxial compression tests). A quasi-static test method that uses crush coupons of simple geometry is proposed to measure the crush stress of composite plies for different fibre orientations and to characterise the associated crushing mechanisms. The experimental results of the crush coupons are then compared to blind predictions from finite element simulations to assess the predictive capabilities of a ply-based material model coupling damage and friction in a continuum damage approach. This material model is currently being developed in parallel to this thesis. Its aim is to pre-emptively simulate structural tests in order to optimise the design of crashworthy structures and to limit the number of physical tests.

Keywords: carbon fibre composite, non-crimp fabric (NCF), mechanical testing, crushing, damage mechanics, finite element analysis (FEA).

Dissertation

This thesis contains a brief review of the research area and summary of the thesis (Part I) and the following appended papers (Part II):

Paper A. Thomas Bru, Peter Hellström, Renaud Gutkin, Dimitra Ramantani and Göran Peterson. Characterisation of the mechanical and fracture properties of a uni-weave carbon fibre/epoxy non-crimp fabric composite. *Data in Brief* **6**, 680–695 (2016).

Paper B. Thomas Bru, Robin Olsson, Renaud Gutkin and Gaurav M Vyas. Use of the Iosipescu test for the identification of shear damage evolution laws of an orthotropic composite. *Composite Structures* **174**, 319–328 (2017).

Paper C. Thomas Bru, Paul Waldenström, Renaud Gutkin, Robin Olsson and Gaurav M Vyas. Development of a test method for evaluating the crushing behaviour of unidirectional laminates. *Journal of Composite Materials* **51**, 4041–4051 (2017).

Paper D. Thomas Bru, Robin Olsson, Gaurav M Vyas and Sérgio Costa. Validation of a novel model for the compressive response of FRP: experiments with different fibre orientations. *In: Proceedings of the 21st International Conference on Composite Materials ICCM-21 (Xi'an, China, 20-25 August 2017).*

Paper E. Sérgio Costa, Thomas Bru, Robin Olsson and André Portugal. Improvement and validation of a physically based model for the shear and transverse crushing of orthotropic composites. Accepted for publication in *Journal of Composite Materials* (September 2018).

Paper F. Thomas Bru, Leif E Asp, Robin Olsson and Gaurav M Vyas. Biaxial transverse compression testing for a fibre reinforced polymer material. *In: Proceedings of the 18th European Conference on Composite Materials ECCM-18 (Athens, Greece, 24-28 June 2018).*

Division of work between authors

Paper A. Thomas Bru performed the through-the-thickness tests and the shear tests. The other tests were performed by the co-authors and the results reported internally at Swerea SICOMP and Volvo GTT. Thomas Bru wrote the paper. Renaud Gutkin proof-read the paper and contributed with suggestions and comments.

Paper B. Thomas Bru performed the experiments, and the numerical simulations with the assistance of Gaurav Vyas and Renaud Gutkin. Thomas Bru wrote the paper. All co-authors contributed with suggestions for the techanical work and the writting of the paper.

Paper C. Thomas Bru assisted MSc student Paul Waldenström in the design of the test and the manufacturing of the specimens, the testing and the post-processing of the results as well as the failure analyses of the specimens. Thomas Bru wrote most of the paper with assistance from the co-authors.

Paper D. Thomas Bru performed most of the tests and established the method to measure the crush stress. Thomas Bru wrote the paper and presented the results at the ICCM-21 conference (oral presentation). All co-authors contributed with suggestions and comments during the writing of the paper.

Paper E. Sérgio Costa developed and implemented the material model. Thomas Bru assisted André Portugal with the numerical simulations of the compression tests and the crush tests. Sérgio Costa and Thomas Bru wrote the paper together. Robin Olsson contributed with suggestions and comments.

Paper F. Robin Olsson suggested the approach. Thomas Bru performed the tests and the post-processing of the data. Thomas Bru wrote the paper and presented the results at the ECCM-18 conference (oral presentation). Leif Asp, Robin Olsson and Gaurav Vyas proof-read the paper and contributed with suggestions and comments.

Contents

Part I

Review and summary of thesis

1 Background

1.1 Composite materials in automotive industry and their use in crash structures

The aerospace industry has now successfully completed a transition period in the substitution of metallic components to composite components, in particular those made of carbon fibre reinforced plastics (CFRPs). However, CFRPs are rarely found outside of luxury and higher performance cars today. Although BMW pioneered the use of CFRPs in the automotive industry with its i3 model in 2013, the first mainstream passenger car with a full composite body in white structure, no other mass market vehicle manufacturers have followed their lead since then.

Thanks to their exceptional specific mechanical properties, CFRPs offer the highest weight reduction potential amongst lightweight materials. Focusing on automotive industry, the key drivers for lightweight solutions are the CO_2 emissions regulation. The average emissions level of a new car sold in Europe in 2017 was 119 grams of CO_2 per kilometre [1]. The 2020 target and (currently proposed) 2025 target are 95 and 81 grams of CO_2 per kilometre, respectively [1]. Considering that 100 kg mass reduction on a passenger car saves between 7.5 to 10 grams of CO_2 per kilometre [2], the upcoming EU targets cannot be achieved with lightweight materials alone. Other CO_2 reduction options, e.g. combustion engine efficiency and hybrid electrified powertrains, will also have to contribute to some extent to fulfil the future regulations. In the case of fully electric vehicles, lightweight materials should not be seen as a measure to reduce CO_2 emissions but as a solution for improving driving range by compensating for the heavy weight of current battery systems. Electric vehicles could also benefit from the introduction of CFRP materials to better protect the battery. The recent report from Automotive World in 2018 [3] predicts that the future of composite materials in automotive may be different to that of aerospace: instead of being used intensively in mainstream vehicles, CFRPs may more likely be used in strategic locations only to reinforce distinct structural components. Also, besides mass reduction, other opportunities offered by composite materials may be taken advantage of. These opportunities, are amongst others, the reduction in assembly complexity, the greater design freedom, the design of multi-functional structures, and the improvement of crash safety.

The potential crash performance improvement offered with composite materials was first revealed through the story behind the McLaren MP4-1 racing car. When it first raced in Formula 1 World Championship in 1981, the McLaren MP4-1 was the first Formula 1 car with a monocoque entirely made of CFRP material. Originally there was scepticism over the capacity of the car to withstand a crash, but an accident at the 1981 Monza Grand Prix proved people wrong. British driver John Watson walked away safely after he crashed his McLaren MP4-1 into the barrier of the Lesmo corners at 230 km/h. Despite the engine and gearbox of the car being torn off, the CFRP monocoque did not “explode into a cloud of black dust” as many sceptics had expected. The McLaren MP4-1 revolutionised the sport and possibly made the

largest single contribution to driver safety of any innovation in the sport's history [4]. Since the second half of the 1980s, all F1 teams are using CFRP monocoques.

Despite the success of composite monocoques in car racing, not even luxury cars that currently boast a CFRP-intense body structure are employing composites for their crash front and rear structures (McLaren 12C, Lamborghini Aventador, Bugatti Veyron). The only exception being the Lexus LF-A supercar that has some crash structures made of carbon fibre composites [5]. The preferred material for front and rear car crash structures is aluminium, not because it necessarily performed better than CFRPs but because the crash behaviour of aluminium structures can be predicted with much higher accuracy than for CFRP structures. Every car launch on the market today must fulfil strict crash safety requirements. In Europe, the safety ratings are attributed by Euro NCAP [6]. Crash performance cannot be compromised and must be evaluated at different stages of the design of a vehicle. Because physical testing is associated with high costs, the assessment of crash structure performance in the automotive industry must intensively rely on numerical tools. However, current models for CFRP materials are not robust enough to give a predictive evaluation of the performance of CFRP structures in crash situations. The following quotes collected during interviews of crash experts for a survey by the U.S Department of Transportation in 2007 [7] highlight the knowledge gaps in predicting the crash performance of CFRP structures:

"There is no basic understanding to predict the performance of automotive structural composites in real crashes."

"There is no correlation between testing of small composite specimens and the crash failure behavior of a full-size vehicle in real crashes."

"Safety standards are written for metal–not composite–vehicles."

1.2 Crushing of CFRP structures and associated energy dissipating failure mechanisms

Car crash structures are designed to fail in a controlled way so that a sufficient amount of the kinetic energy is absorbed by the structure in a crash event to decelerate the car and to limit the load transmitted to the occupants. The failure mode of impacted car structures can be divided into two categories: bending dominated failure (e.g. B-pillar and roof) and axial compression dominated failure (e.g. crash boxes in front and rear assembly). Axial compression is the most efficient design for energy absorption, at the condition that progressive failure by controlled collapse of the structure is achieved and catastrophic failure is avoided. Fig. 1 illustrates the catastrophic and progressive failure modes of a CFRP structure subjected to axial loading. The typical load–displacement curve of the progressive failure mode is characterised by an initial peak load, immediately followed by a sustained crush load plateau (P_s in Fig. 1) as the crush zone propagates along the structure. The total energy absorbed by the crash structure is represented by the area under the load–displacement curve.

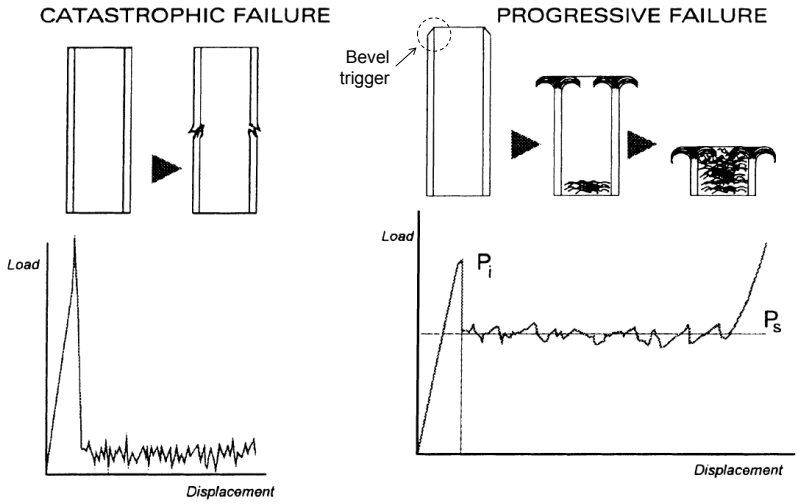

Figure 1: Catastrophic failure versus progressive failure (crushing) of a composite structure; after [8].

From Fig. 1, it is evident than the energy absorption is considerably higher in the case of crushing failure than in the case of catastrophic failure. The specific energy absorption (SEA) is defined as the ratio of total energy absorbed over the mass of crush material. It is often used to compare the crashworthiness of different energy absorbing structures. The range of SEA values reported in the literature for composite crash structures is 50-180 $\mathrm{kJ\,kg^{-1}}$ [9]. For comparison, the range of SEA for metallic crash structures is 30-90 $\mathrm{kJ\,kg^{-1}}$ [9]. Even though the range of SEA for composite structures is extremely wide, it still indicates that higher SEA, and therefore improved crash performance, can potentially be achieved by replacing metals with CFRP materials. The large variation in SEA reported in the literature, even for similar material systems, emphasises the fact that there are many factors which control the energy absorption capability of composites. Some of these factors are the structural geometry, its lay-up (i.e. the arrangement of the fibres), and the loading rate at which it is being crushed, etc. [9]. As a result, the SEA should not be considered as an intrinsic material property and should only be used in like-with-like comparison to rank material energy absorption capabilities.

The stable collapse modes of CFRP structures subjected to axial loading are considerably different from those observed in metallic structures. The brittle nature of composite material ensures than the dominant mechanism is that of fracture/crack formation. On the contrary, the ductile nature of metals yield a collapse of metallic crash structures by progressive buckling and local bending. The crushing modes of composite structures is characterised by the formation of a stable zone of microfracture (crush zone) that propagates at a rate approximating the compression rate. As for SEA, the crush zone morphology and the sequence of the different microcraking mechanisms involved in the process are sensitive to changes in material system, specimen geometry, and testing conditions. A conceptual representation of the crush zone for a CFRP crash tube is shown in Fig. 2. The main features that can be identified are:

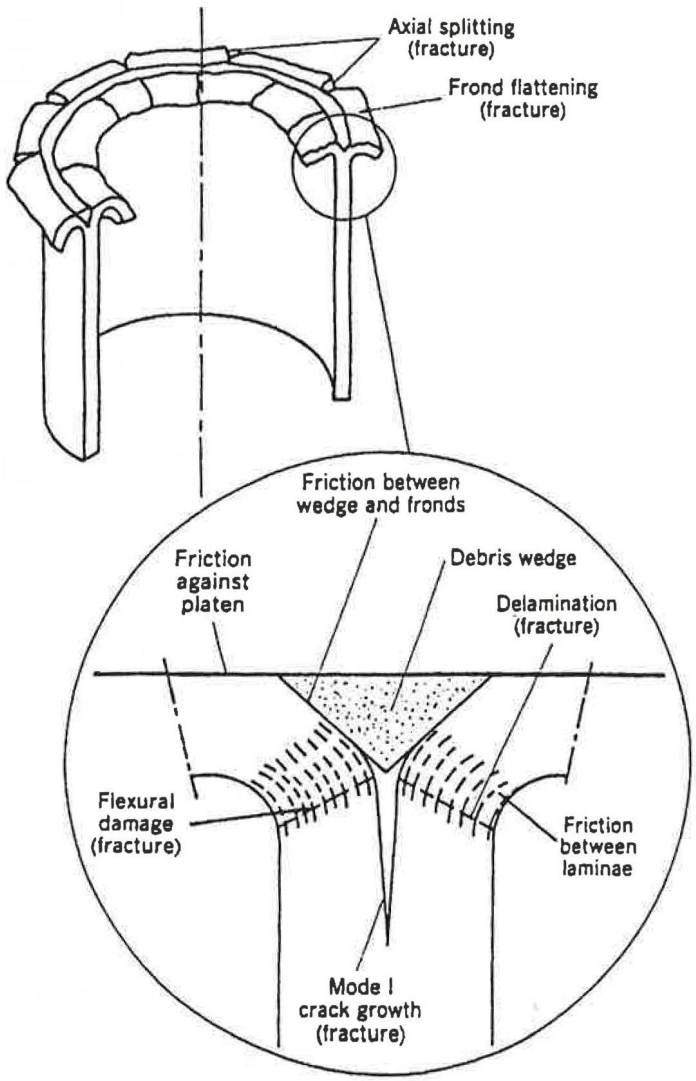

Figure 2: Schematic representation of the crush zone morphology for a CFRP tube subjected to axial loading [9].

- two sub-laminates experiencing bending deformation inwards and outwards of the tube (splayed lamina or fronds),
- a severely strained zone in the highly curved region of the splayed lamina responsible for flexural damage across the sub-laminates and delamination failure (ply separation),
- a deep axial crack ahead of the crush zone,
- a debris wedge of fragmented material that is being pushed down during the crushing process.

Fragmentation and splaying have been identified by Hull [10] as the two extreme crushing modes of CFRP structures, see Fig. 3. In the fragmentation mode, a brittle

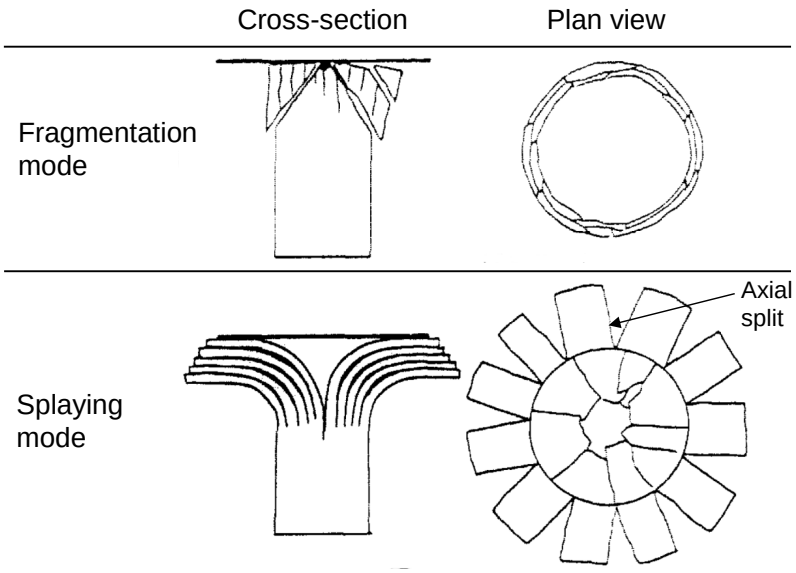

Figure 3: Schematic representation of the fragmentation crushing mode and the splaying crushing mode for a CFRP tube; after [10].

failure is observed with multiple inclined cracks breaking the material into debris. In the splaying mode, delamination cracks are forcing the material to bend/splay extensively into continuous fronds with no or few amount of flexural damage (thanks to the large radius of curvature of the splayed lamina). The presence of axial splits in the fronds are evidence that even tensile failure must be considered in crash scenarios. In most cases, the crushing mode is a combination of both fragmentation and splaying, as in the representation given in Fig. 2. The debris wedge on top of the crush zone is a result of the fragmentation crushing mode, while the flexural damage and the mode I crack growth are results of the splaying crushing mode.

From Fig. 2 and Fig. 3, the following sources of energy dissipation during progressive collapse of CFRP structure may be listed:

- fracturing of the splayed lamina (axial splits, flexural damage, delamination),
- fragmentation of the material into the debris wedge,
- crack growth ahead of the crush zone,
- frictional resistance to the penetration of the debris wedge,
- frictional resistance to the sliding of delaminated surfaces and other fracture surfaces,
- frictional resistance to the composite material sliding across the crushing plate (the crushing plate, usually made of steel, is used to introduce the compressive loading in the structure),

and may be divided into energy dissipated by damage mechanisms and energy dissipated by friction. The damage mechanisms, or failure modes, of continuous fibre

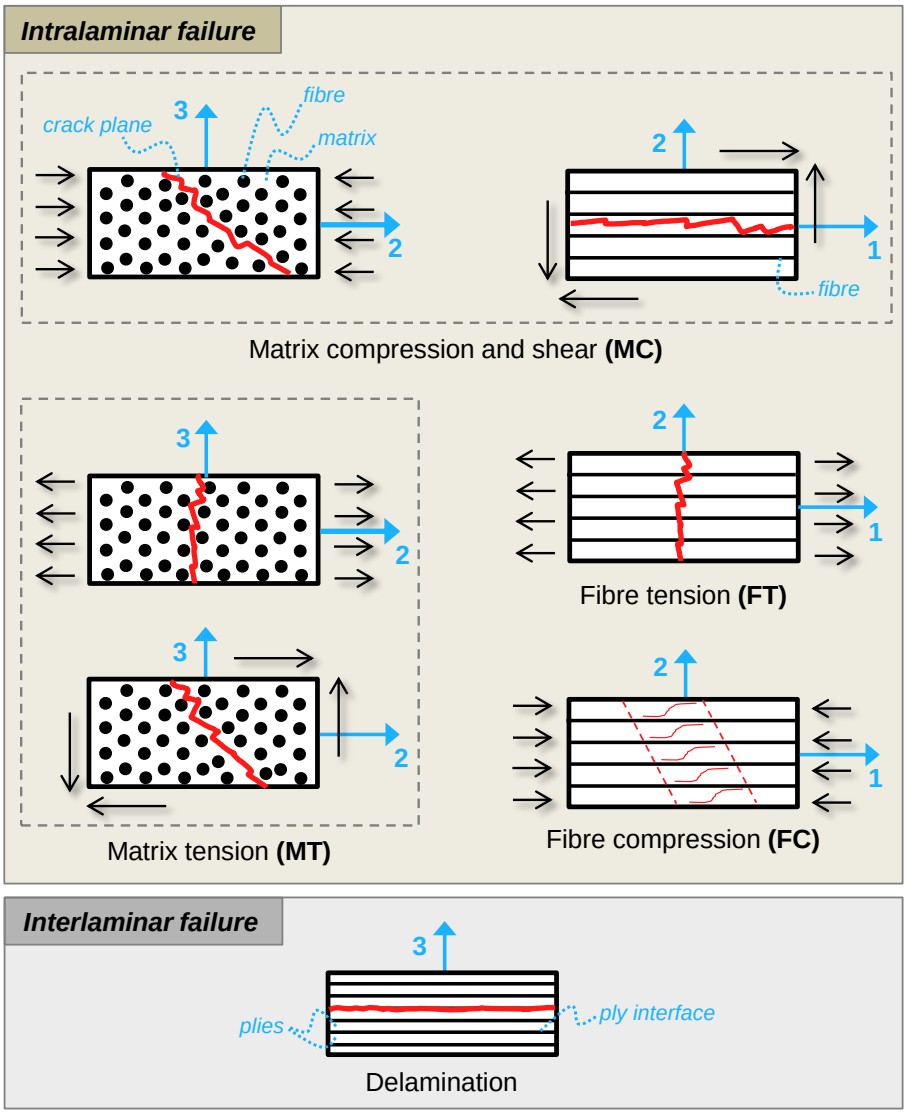

Figure 4: Energy dissipating failure mechanisms of continuous fibre composite materials in crash scenario.

laminates include *intra*laminar failure (failure *within* a ply) and *inter*laminar failure (failure *between* plies). The different failure modes and associated crack planes, or failure planes, are illustrated in Fig. 4. The nature of the matrix and fibre constituent of the composite material and the local three-dimensional stress state in the structure are influencing the complex sequence of failure mechanisms involved in the process of composites undergoing crushing.

Breaking down the individual contributions of the different sources of energy dissipation involved in crash of composites is a challenge. Experimentally, only the total energy absorption in a crash structure can be measured directly with standard equipment. Unless individual damage modes are isolated from each other, it is not possible to evaluate the energy absorption associated with each of the damage mechanisms. Numerical simulation using finite element (FE) methods must be used

Table 1: Specific energy absorption (SEA) break down in $[0/90]_{3s}$ carbon fibre/PEKK corrugated specimens; data extracted from [11].

	Experiments	**Numerical simulation**	
	SEA ($kJ\,kg^{-1}$)	SEA ($kJ\,kg^{-1}$)	Percentage of total SEA
Total	110.1	109.9	100%
Fibre failure (FC, FT)	-	36.9	34%
Matrix failure (MC, MT)	-	27.2	25%
Friction	-	19.9	18%
Delamination	-	13.0	12%
Viscous effect	-	7.6	7%

for that purpose. The simulation results by Tan & Falzon [11], reported in Table 1, indicate that intralaminar failure was the major contributor to the measured energy absorption for the particular crash structure investigated. Fibre compression (FC), fibre tension (FT), matrix compression/shear (MC) and matrix tension (MT) damage were responsible for nearly 60% of the overall SEA. The energy dissipated by friction was the second most important contribution to the total energy absorption of the structure (less than 20% of the total SEA). Finally, the propagation of delaminations (interlaminar cracks) in the structure was found to contribute for slightly more than 10% of the total SEA. The viscous energy dissipation (less than 10% of the total SEA) is due to the use of damping methods in explicit dynamic simulations. It is worth mentioning the results in Table 1 are sensitive to the modelling strategy used in the study to represent failure and they are only reported here to give the reader an insight into a possible energy absorption break down during crushing of a composite structure. Also, the values reported in Table 1 are only valid for the particular crushing mode reported in [11]. For instance, if the $[0/90]_{3s}$ specimen lay-up is changed so that the amount 0°-fibres increases and that the amount of fibre compressive failure with respect to the other failure modes also increases, then the SEA value associated with the fibre failure mode would most likely be higher than the reported value of 33.7 $kJ\,kg^{-1}$.

1.3 Measurement of mechanical properties relevant for crash analysis

Experimental characterisation refers to the determination of the material properties through tests conducted on suitably designed specimens. For simplicity, the tests usually consist of the loading of flat specimens under quasi-static conditions in a universal testing machine. The common practice is to evaluate the material properties associated with a single ply using unidirectional UD test specimens and then use laminate theory to calculate the properties of laminates.

Elastic constants and strengths constitute basic mechanical properties of CFRP

Table 2: Material characterisation tests for the determination of ply properties, interlaminar fracture toughness and intralaminar fracture toughness. (Refs.= ASTM standards or relevant publications)

Test method		**Properties**	**Refs.**
Uniaxial tension	In-plane	E_{11}, E_{22}, ν_{12}, X_t, Y_t	[12]
	Through-thickness*	E_{33}, ν_{32}, Z_t	[13]
Uniaxial compression	In-plane	E_{11}, E_{22}, ν_{12}, X_c, Y_c	[14, 15]
	Through-thickness*	E_{33}, ν_{32}, Z_c	[13]
Shear	In-plane	G_{12}, S_{12}	[16–19]
	Through-thickness (1–3)	G_{13}, S_{13}	[18–21]
Fracture toughness	Delamination	G_{Ic}, G_{IIc}, $G_{I/IIc}$	[22–24]
	Fibre failure*	G_c^{ft}, G_c^{fc}	[25, 26]

* No standard test method available for these tests.

plies. The in-plane properties can be determined through standardised quasi-static uniaxial tension, uniaxial compression and shear test methods, as reported in Table 2. For shear, the response is known to exhibit nonlinearity so the entire stress-strain curve must be evaluated. In Table 2, the index 1 denotes the fibre direction, 2 denotes the in-plane transverse direction and 3 denotes the through-thickness direction. Dedicated through-thickness tests are necessary for orthotropic plies (i.e. plies with different properties in the 2– and 3–directions). Through-thickness tests are not necessarily documented with test standards. In addition to the basic mechanical properties, fracture toughness properties (i.e. the material resistance to crack growth) are relevant for crash applications. The measurement of the different fracture toughnesses associated with delamination (interlaminar failure) of UD laminates is relatively well established today [27]. However, the evaluation of the energy release rate of intralaminar failure modes (cracks in a ply between fibres and cracks breaking fibres) have received less attention and these properties are still today difficult to measure. This is unfortunate, particularly considering the high energy associated with the fibre failure modes in CFRP crash structures (c.f. Table 1).

Crash events imply dynamic deformation of structures and materials. Because they are simple and easy to control, quasi-static tests are often preferred for material characterisation and for the evaluation of energy absorption capabilities of crash structures. However, quasi-static tests may not be a true representation of the actual crash conditions since many CFRP materials are strain rate sensitive. The extensive experimental test campaign by Koerber *et al.* [28–31] highlights that stiffness, strength and fracture toughness properties of carbon/epoxy composites (IM7/8552 material system) are strain rate sensitive. Specimens were tested for transverse compression, in-plane shear, longitudinal compression and intralaminar fracture toughness, in quasi-static conditions and at high strain rate using a split-Hopkinson pressure bar (the strain rate varied between 60 to 360 s^{-1} depending on the test). The results show that, from quasi-static loading to dynamic loading, the

transverse compressive strength (Y_c) increases by 45%, the in-plane shear strength (S_{12}) increases by 42%, the longitudinal compressive strength (X_c) increases by 38%, the intralaminar fracture toughness associated with fibre compression (G_c^{fc}) increases by 63% and the intralaminar fracture toughness associated with fibre tension (G_c^{ft}) increases by 19%. An increase of the elastic moduli E_{22} and G_{12} of about 10 to 20% was also observed in high strain rate tests. Regarding crushing of composite structures, there is a lack of consensus in the literature about the influence of test speed on the energy absorption. As reported in the review by Jacob *et al.* [32], some researchers observed an increase of the SEA with an increasing crushing speed, others a decrease of SEA, and others no variation of SEA with crushing speed. Only one thing is certain, that if the mechanical response of the damage mechanisms involved during crushing is a function of strain rate and/or if the frictional forces generated during crushing is a function of strain rate, then the energy absorption of CFRP structures will be a function of the testing speed.

1.4 Available models for composite crash simulations

FE methods have been widely used to simulate the performance of CFRP crash structures. Many material composite models are available today across the explicit FE codes PAM CRASH, LS-DYNA and ABAQUS. ABAQUS CZone technology [33] is used by several Formula 1 teams for the analysis of large and complex CFRP crash structures [5]. The CZone technology is based on an empirical model which requires the performance of carefully designed crush experiments on material coupons. An algorithm is then able to interpolate the crush behaviour for different designs from the crush loads measured in the calibration experiments. Unlike such empirical models, other models attempt to capture the detailed behaviour (to some extent) of the crushing phenomenon by modelling the individual sources of energy dissipation. The recent damage models developed by Tan & Falzon [11] and by McGregor *et al.* [34] for crashworthiness predictions of composite structures fall in this category. Although not intended for crash originally, the material models MAT054, MAT058 and MAT262 implemented in LS-DYNA [35] have been widely used for crash modelling of composites in recent years. The main characteristics of these three models are presented hereafter and their predictive capabilities are discussed.

MAT054, MAT058 and MAT262 are ply-based models consisting of a linear elastic material model, a set of failure criteria and a degradation scheme. The failure criteria predict the initiation of damage in a ply, while the degradation scheme describes the post failure behaviour of that ply. The post failure behaviour is characterised by a softening response during which one or several stress components are degraded, thus capturing the stiffness degradation of the damaged material. The post failure response ends at element deletion/erosion, the point at which the finite element is removed totally from the simulation. MAT054 uses the Chang-Chang failure criteria for failure initiation and a failure model with no softening in its degradation scheme. When the failure condition is fulfilled in a given ply, the ply properties are immediately dropped to zero or to a constant value. MAT058 uses a modified Hashin

Table 3: Number of input parameters for different composite material models in LS-DYNA [35].

Material model:	MAT054	MAT058	MAT262
Total number of variables	42[a]/60[b]	49	51
Material parameters	16[a]/16[b]	21	24
Non-physical parameters	10[a]/22[b]	11	7

[a]Excluding the optional material cards
[b]Including the optional material cards

set of failure criteria and a continuum damage mechanics (CDM) approach with nonlinear softening. Using a CDM approach allows for a progressive degradation of the stress components during the post failure behaviour, as opposed to the immediate stress degradation in MAT054. Finally, MAT262 uses LaRC04 [36] failure criteria for the failure initiation and a CDM approach with linear or bilinear softening (depending of the failure mode) upon failure initiation.

MAT054, MAT058 and MAT262 require a different number of input parameters, see Table 3. The models are formulated in terms of material parameters, which are measurable mechanical properties, and in terms of non-physical parameters, which are either purely mathematical expedients or cannot be measured experimentally. The material parameters include the different ply stiffness and strengths as well as the nonlinear in-plane stress–strain shear behaviour. These parameters can be extracted for a given material system following standard test protocols (c.f. Section 1.3). MAT262 uses intralaminar fracture toughness values for modelling the post failure behaviour, and therefore requires a more extensive material characterisation than the two other material models. It is evident from Table 3 that a large number of non-physical parameters are required for all models. Unfortunately, there is no way to measure these parameters nor to relate them to material properties.

Several studies in the literature [37–39] have shown that the non-physical parameters in MAT054, MAT058 and MAT262 considerably affect the results of composite crash simulations. Although it may be possible to reproduce the experimental load–displacement curves in the simulations, all models require extensive parameter tuning in order to achieve a good correlation with the experimental data. Cherniaev *et al.* [38] concluded that "without calibration, using default or recommended values for the non-physical parameters can result in erroneous representation of composite crushing". Cherniaev *et al.* [38] and Feraboli *et al.* [39] showed that the crash front softening factor (SOFT parameter), which is common to the three material models, is the single most influential parameter in the FE simulations. Because its value cannot be determined *a priori* but only by trial-and-error, simulations using any of these three material models should not be regarded as fully predictive. Additionally, mesh size and filtering scheme can also influence the results of crash simulations [39].

2 Aims and scope

While experimental full-scale crash testing remains an integral part of safety and certification in the industry, the procedure is extremely expensive and time consuming. Because automotive is a cost-driven industry, it must rely on the capability of FE codes to pre-emptively simulate structural tests in order to optimise the design of crashworthy structures and to limit the number of physical tests. This strategy is well-known from the aerospace industry as the building block approach design [40]. As illustrated with the Rouchon Pyramid in Fig. 5, the idea behind the building block approach is to build knowledge on the material and structural behaviours step by step, starting from the fundamental stage at the coupon level up to the full scale structure.

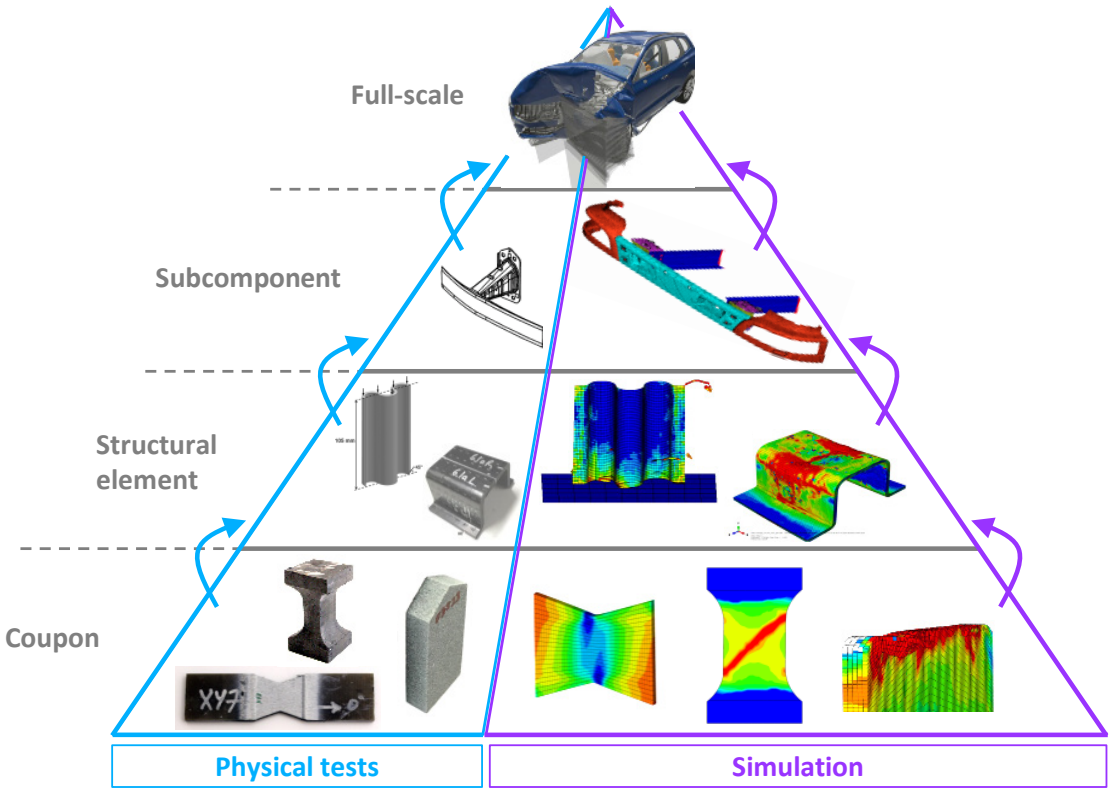

Figure 5: The building block approach applied to automotive composite crash structures.

FE simulation is an important companion of the physical tests in the building block approach (Fig. 5). Simulation can replace some physical tests, with the condition that the FE analyses are predictive. As mentioned previously, there is not yet any reliable FE tool to predict the energy absorption capability of a composite structure with an arbitrary lay-up, which is a hindrance to the introduction of composite materials in mass-produced cars. The great challenge presented by the simulation of CFRP crash structures is the complex nature of the combination of individual failure mechanisms occurring during the process of damage. The different sources

of energy dissipating mechanisms must be captured accurately for the simulation to be predictive, which implies the knowledge of the different failure mechanisms during crushing of a particular composite material and structure. The predictive capability of the simulations is also greatly relying on the quality of the input model parameters extracted or calibrated from experiments. Finally, an efficient model formulation and implementation in a FE scheme are needed to allow the computation of large composite structures in a reasonable amount of time[1]. These experimental and numerical aspects of composites in crash events are illustrated in the suggested research road map in Fig. 6.

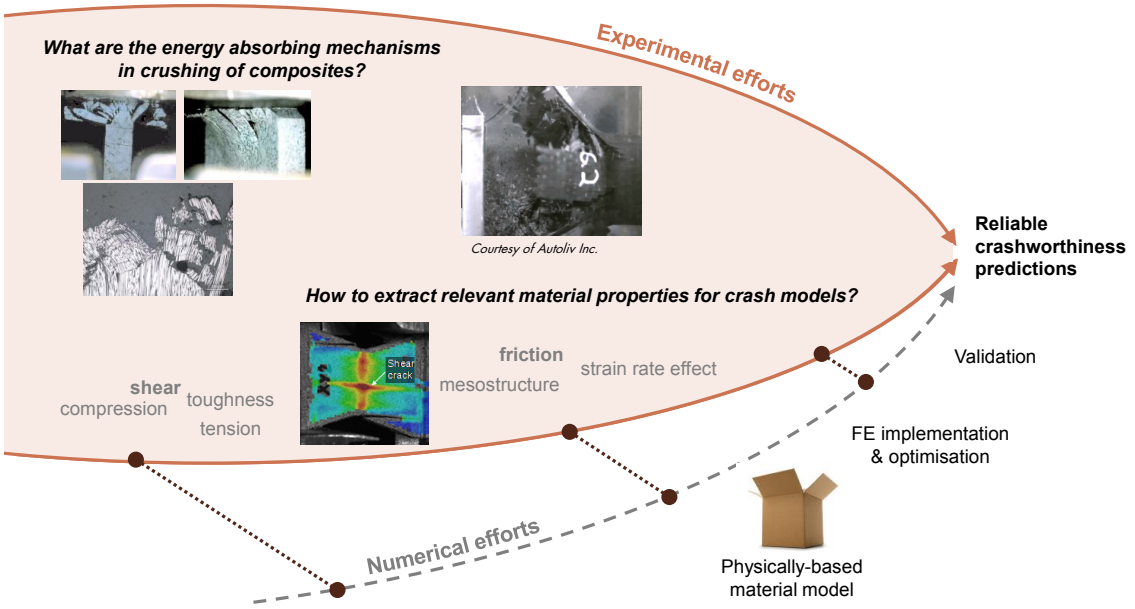

Figure 6: The experimental road map towards predictive computational models for composites in crash situation.

The experimental work related to the road map in Fig. 6 and that are covered in this thesis consist of:

- the identification and understanding of the key failure mechanisms in crushing that are to be included in the material model formulation,
- the extraction of relevant material properties for crash modelling from experiments,
- the development of crush tests which can be simulated relatively easily in order to support the development and the validation of the FE codes (i.e. tests associated with the first stage of the building block approach pyramid).

This thesis does not aim at investigating different composite materials to compare their energy absorption capabilities. Only one CFRP material is studied in detail

[1]Current full car models for crash simulations consist of approximately 10 millions elements and take about 30 hours to run [41].

in this work (c.f. Section 3). This thesis does not aim either at investigating experimentally the crash performance of real energy absorbing structures, like the full front assembly of a car for instance (i.e. tests associated with the higher stages of the building block pyramid). Instead, small coupons are tested experimentally and compared to model prediction, as a part of an early validation step of a building block approach with increasing structural complexity. Finally, strain rate effects are not investigated in this thesis. The test methods developed in this work to determine the material parameters to input to the model are quasi-static test methods and cannot be directly used in dynamic conditions. Similarly, the crash experiments at the coupon level developed for the understanding of the key failure mechanisms in CFRP crash were only performed at a quasi-static strain rate.

The numerical efforts mentioned in Fig. 6 include (i) the development of a physically-based ply model for crash, and (ii) the improvements of the computational efficiency of crash simulations. Those two research topics are being addressed as part of the projects "Modelling crash behaviour in future lightweight composite vehicles – FFI1/2" [42] and "Reliable crash modelling of fibre composites for lightweight vehicles – compcrash2" [43], which are carried out with a strong interaction with the research presented in this thesis. The physically-based ply damage model for crash is briefly described in Section 4. Regarding the improvement of the computational efficiency of crash simulations, the challenge consists of using a relatively simple finite element formulation to keep the computation time low, while at the same time correctly capturing the local three-dimensional stress state in the material to accurately predict intralaminar and interlaminar failure [44].

3 Material system selected for the study

The CFRP reinforcement characterised in this work is a 205 gsm uni-weave non-crimp fabric (NCF) style 4510 from Porcher Industries [45]. The carbon fibre bundles are Tenax®-E HTS45 E23 12K. The bundles are held together by glass fibre/polyamide weft threads, visible in Fig. 7. The thermoset epoxy resin is Araldite® LY 556 / Aradur® 917 / Accelerator DY 070 from Huntsman [46]. In this thesis, the composite laminates made from the NCF reinforcements and the epoxy resin mentioned above are sometimes referred to as "HTS45/LY556 composites" for simplicity.

NCF are textile reinforcements made of one or several layers of parallel fibre bundles stacked on top of each other and held together with threads. If the fabric only contains one layer of parallel bundles woven together with thin weft threads, then the reinforcement is denoted as uni-weave NCF. A comparison of the ply architecture of a composite reinforced with a UD prepreg tape and a composite reinforced with uni-weave NCF is given in Fig. 8. Unlike in the prepreg composite, the uni-weave NCF exhibits through-thickness fibre waviness and resin-rich areas between bundles. For these reasons a UD ply of NCF cannot be approximated as transversely isotropic perpendicular to the fibres and should be treated as an orthotropic ply.

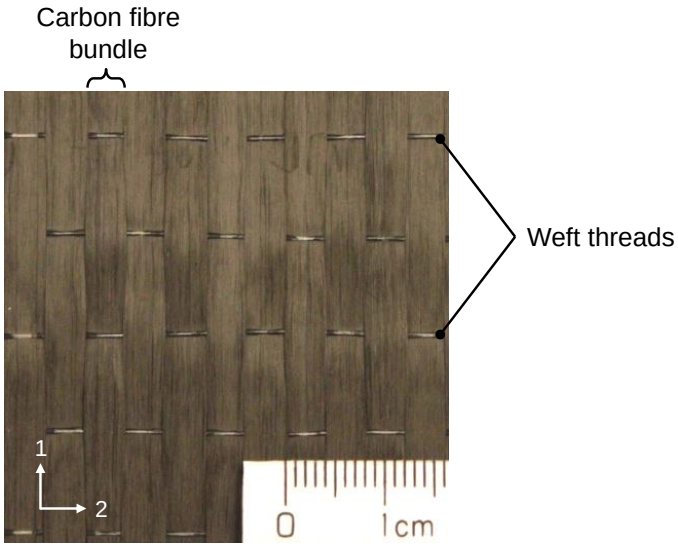

Figure 7: Photograph of the HTS45/LY556 uni-weave NCF reinforcement, from **Paper A**.

CFRP prepregs are used extensively in the aerospace industry, despite their high costs and slow manufacturing process (autoclave process). However, hand lay-up and autoclave need to be abandoned to achieve the high production rate in the automotive industry[2]. Textile reinforcements can be used in out-of-autoclave processing techniques, which are in general much faster than the autoclave process. Processing times vary for different manufacturing methods and polymer resins, but the manufacturing of composites can be reduced to a few minutes when using fast curing thermoset epoxy resins, and can get even faster when using thermoplastic polymers.

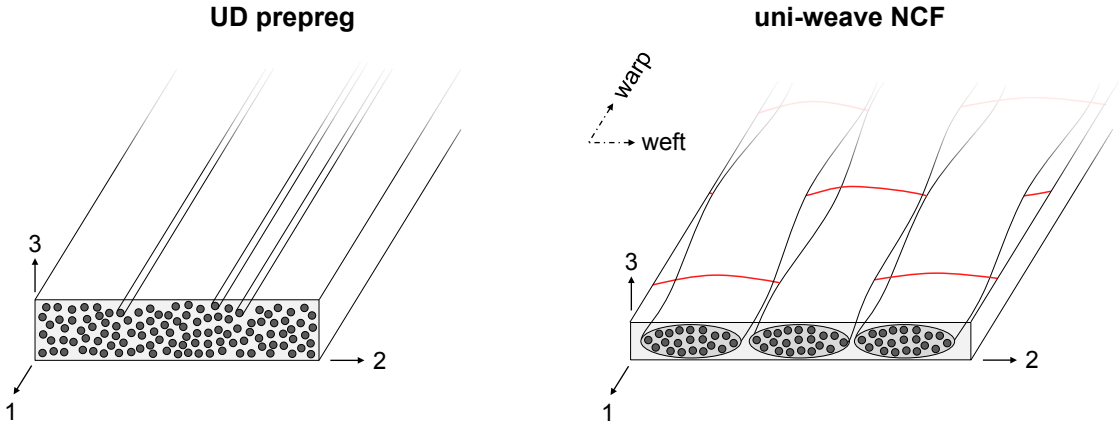

Figure 8: Illustration of a UD prepreg ply and a uni-weave NCF ply with weft threads.

The degree of through-thickness waviness (or crimp) in NCFs is low in compar-

[2]In 2017, Volkswagen Group produced more than 10 millions cars while Boeing only produced 763 aircraft [3].

ison to other textile reinforcements, thanks to the large difference in aspect ratio between the weft threads and the bundles. Crimp ultimately results in a loss of in-plane mechanical properties of the final laminate in comparison to prepreg. The experimental study by Wilhelmsson *et al.* [47] on several HTS45/LY556 uni-weave NCF laminates with various amount of crimp showed that the loss in compressive stiffness E_{11c} is controlled by the *mean* crimp angle in the laminate, while the loss in compressive strength X_c is controlled by the *maximum* crimp angle that exists locally somewhere in the laminate.

Besides introducing crimp, the threads in NCFs may also affect the laminate failure modes. In **Paper B**, it was found that the failure of UD laminates under 1–3 shear was interlaminar and it initiated at the weft threads of the fabric. In **Paper C** and **Paper D**, it was observed that the clustering of weft threads through the thickness of UD laminates was promoting splaying failure over fragmentation during longitudinal crushing.

4 Ply-based damage model selected for the study

The experimental part of this thesis is towards supporting the development and the validation of the material model for crush of CFRPs initially developed by Gutkin & Pinho [48] and later extended by Costa *et al.* [49, 50]. The ply-based model accounts for all the intralaminar failure modes represented in Fig. 4. The model formulation and its FE implementation are detailed in [48–50] and **Paper E**, so only some relevant features of the model are presented hereafter to guide the reader.

The most relevant failure modes for crash application are the compression failure modes (matrix compression/shear and fibre compression). The model uses a common approach for all compression failure modes. The other failure modes (matrix tension and fibre tension) are not discussed here.

The model uses a CDM approach combined with a friction model to predict the stress–strain response of the ply beyond damage initiation and peak stress, shown in Fig. 9. By combining damage and friction two distinct energy dissipating mechanisms are accounted for in a physical sense: the energy spent to create cracks (damage) and the resistance to the sliding of the crack surfaces (friction). The damage initiation, at the end of the linear region in Fig. 9, represents the nucleation of matrix microscopic cracks. At damage initiation a potential failure plane is defined and the relation between stresses and strains is obtained from the response in that plane. The orientation of the failure plane is set at damage initiation and is fixed during damage growth. The nonlinear response upon damage initiation is the result of damage evolution and increasing forces that arise from the friction between microcrack surfaces. The point at which the ply is fully damaged corresponds to the peak stress. The fully damaged state represents the final failure and is associated to a macroscopic crack across the entire ply. The only load that the fully damaged material can carry in compression beyond the peak stress is the one associated to the frictional resistance to the sliding of the macrocrack surfaces.

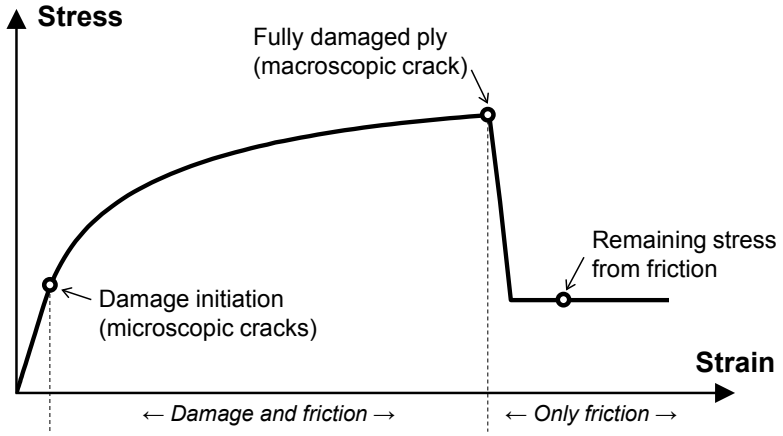

Figure 9: Representative stress–strain response for the material model combining damage and friction.

Using damage to predict the nonlinear material response up to the peak stress is based on physical observations. For transverse compression, bands of microscopic damage are found in the matrix just before the peak stress is reached [51]. For in-plane shear, it has been observed that the shear cusps (features visible on shear failure surfaces) originally initiate from microcracks in resin-rich regions between fibres [52]. For fibre compression, the triggering mechanism for kink-band formation has been found to be the microcracking of the surrounding matrix near the fibres [53]. The damaged matrix is then unable to support the fibres during the compressive loading, which eventually leads to the rotation and the failure of the fibres in a kink-band. Fibre compression is therefore treated as a matrix failure mode in the model formulation[3].

The CDM formulation requires the shear response of the material to be known. The friction parameters are identified together with the damage parameters from experimental shear stress-strain curves. The characterisation of the shear behaviour of the material investigated in this thesis and the model parameters identification from the experimental results are reported in Section 5. A major advantage of the model is that is does not require the measurement of the intralaminar fracture toughness associated with shear, transverse compression and fibre compression failure, which are difficult to extract from experiments.

5 Shear characterisation

Several compressive failure mechanisms in CFRP plies are driven by the shearing of the matrix polymer, which justifies the need for an accurate shear characterisation. In transverse compression, the orientation of the fracture plane indicates the presence of shear forces acting on that plane [54]. In longitudinal compression, failure by fibre

[3]It is the case in [49, 50], but not in **Paper E** which does not include a kinking model for the fibre compression failure mode.

kinking originally initiates from microcracking of the surrounding matrix material which undergoes shear deformation [53].

Pure shear loading of UD plies can be applied either in the 1–2, 1–3 or 2–3 material planes. The in-plane shear response (1–2 shear) and the 1–3 through-thickness shear response can be assumed similar for transversely isotropic plies, but not for orthotropic plies. Applying a pure 2–3 through-thickness shear loading does not lead to a shear failure but to a tensile failure in a plane inclined approximately 45° to the action plane of the shear stresses. A direct 2–3 shear test is therefore not a relevant test for shear material characterisation. Its only interest is the measurement of the elastic modulus G_{23}.

Failure along a closed matrix plane inclined with the angle α with respect to the 3–direction, shown in Fig. 10, is often observed for an external stress state $(\sigma_{11}, \sigma_{22}, \sigma_{33}, \tau_{23}, \tau_{13}, \tau_{12})$ dominated by compressive σ_{22} or σ_{33} stresses or by τ_{23} shear stresses. The external stresses can be resolved in the (potential) failure plane into a normal stress (pressure $\sigma_N \leq 0$) and two shear stresses (longitudinal shear τ_L and transverse shear τ_T) using stress transformation equations. The longitudinal shear stress τ_L is equal to the in-plane shear stress τ_{12} for $\alpha = 0$, which is the case when the material is under a pure 1–2 shear stress. The measurement of the transverse shear response, τ_T versus γ_T, is relevant for the damage model presented in Section 4. This response can be measured indirectly from a test in which the external stress state $(\sigma_{11}, \sigma_{22}, \sigma_{33}, \tau_{23}, \tau_{13}, \tau_{12})$ results in a shear driven matrix failure as explained later.

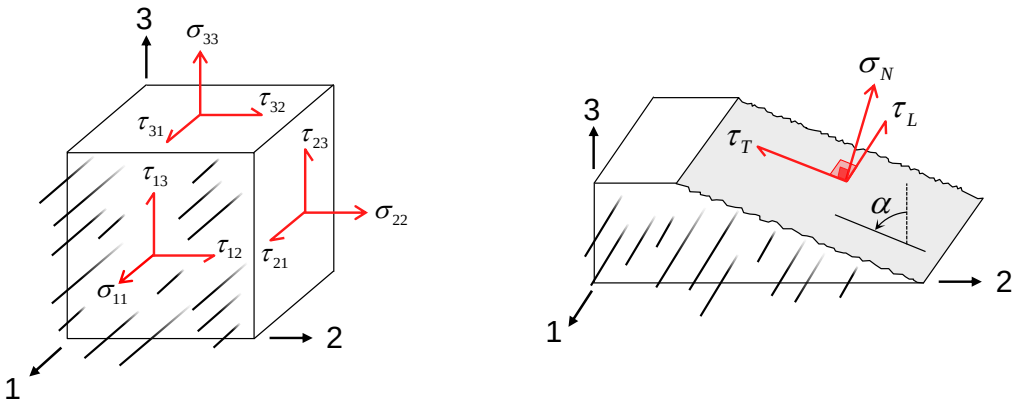

Figure 10: External stresses acting on a UD composite and $(\sigma_N, \tau_L, \tau_T)$ stresses on a matrix failure plane.

The Iosipescu shear test, presented in Section 5.1, was selected for the evaluation of the 1–2 and 1–3 shear responses of the CFRP material investigated in this thesis. For the evaluation of the transverse shear response in Section 5.2, uniaxial and biaxial transverse compression tests were performed to extract the τ_T–γ_T response on the potential matrix failure plane. The shear responses measured from the shear and compression tests can then be used to calibrate the ply-based damage model of interest for this thesis, as described in Section 5.3.

5.1 Iosipescu shear tests

There are currently more than ten test methods to investigate shear behaviour of composite materials. Unfortunately, some of these test methods are far from producing a pure shear stress state and a uniform shear stress distribution in the specimen, which is a requirement for an accurate shear characterisation. For in-plane shear characterisation, the most popular test is perhaps the ±45° tensile shear test [17]. However, the primary virtue of the ±45° tensile shear test is its ease of use and not the quality of the results produced. Because the stress state in the specimen is complex and far from being pure shear it is not a reliable quantitative test and should only be used for shear modulus evaluation [55]. For interlaminar shear characterisation, which is relevant when investigating delamination, the short beam shear test is ranked first in frequency of use [56]. Again, it is not possible to relate the short-beam strength to any one material property because of the complex stress state in the specimen. Because it is easy to perform, the short beam shear test is anyway a good candidate for material screening and quality control tests. When comparing the different shear test methods available for different type of composites, the Iosipescu shear test is often ranked among the top places [52, 57]. The notoriety of the Iosipescu test method is due to the high quality of the data produced and the possibility—at least in theory— to evaluate all three shear stress states. In reality, 2–3 shear tests with Iosipescu specimens only give shear modulus measurements because of a catastrophic tensile failure occurring outside the test region at relatively low loads [58]. Therefore, for UD composites, only the entire 1–2 and 1–3 material shear responses can be evaluated with Iosipescu specimens.

Since it was initially proposed by N. Iosipescu in 1967, only two reviews on the Iosipescu test as applied to composite materials appeared to have been published in the literature. The review by Adams & Walrath [59] served as a basis for establishing the ASTM standard D5379 in 1993 [18]. In 2018, Stojcevski *et al.* [56] provided an update on the current status of the Iosipescu testing as well as an extensive catalogue of the research history in that field. Within the scope of this research project, the author also preformed a literature review of the Iosipescu test [60].

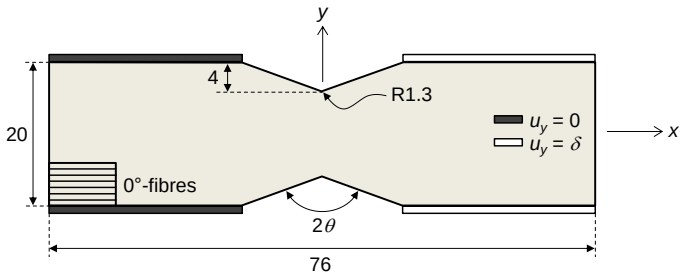

Figure 11: Iosipescu shear specimen (dimensions in mm).

The Iosipescu test principle is the asymmetric four-point bending of a V-notched specimen. The loading is achieved through the Wyoming fixture by introducing a compressive load at one end of the specimen while holding the other end fixed (Fig. 11). Theoretically, a pure stress state with zero bending moment is created

through the center of the specimen (the y–axis in Fig. 11). The sharp change of geometry in the specimen introduces unavoidable stress concentrations at the notch tip. The shear stress concentration factor is minimized when using a notch root radius of 1.3 mm [61]. To achieve a uniform shear stress distribution, the notch depth to specimen height ratio should be around 20% and the notch angle 2θ should be scaled from the orthotropy ratio of the laminate investigated [62]. An improved version of the Wyoming fixture was proposed by Melin [63] to avoid the formation of a stress gradient through the thickness of the specimen as a result of an out-of-plane specimen rotation during testing. An in-house Iosipescu fixture inspired from the design proposed by Melin [63] was used for the shear tests presented in this thesis.

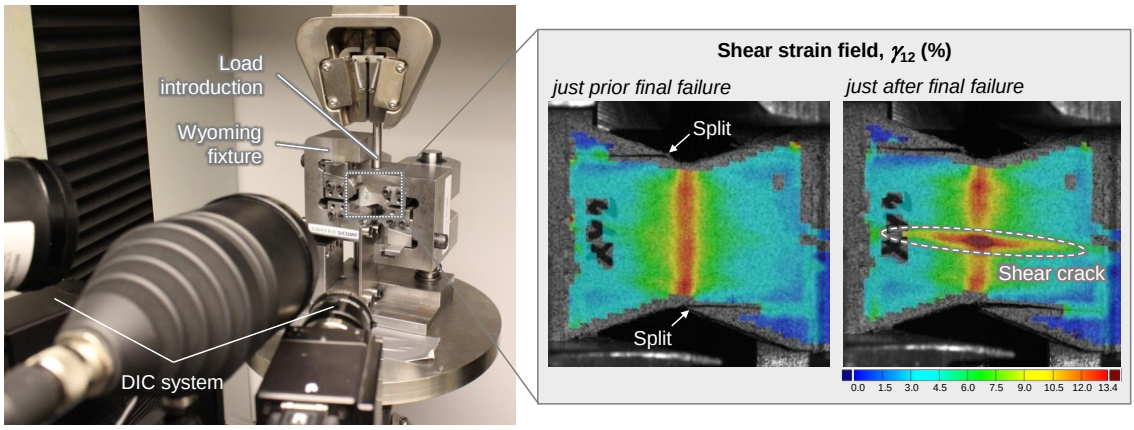

Figure 12: Shear strain field measured experimentally in a Iosipescu specimen, from **Paper B**.

In **Paper B**, the quality of the Iosipescu shear specimen is assessed experimentally with full-field strain measurements using the digital image correlation (DIC) method and numerically with an FE analysis for the carbon/epoxy uni-weave material studied in this thesis. The strain state (and therefore stress state as well) is optimal for theoretical research: a relatively pure shear strain and a uniform shear strain distribution are found in the central region of the specimen, as shown in Fig. 12. Most of the test specimens failed prematurely by longitudinal splitting at the notches prior to final shear failure between the notches. This premature failure has been observed by many when testing thermoset UD composites [56] and is due to transverse tensile stresses along the specimen notch flanks. Although not detrimental to the shear stress uniformity, splitting failure is responsible for introducing unwanted transverse stresses in the specimen. The strain readings from the DIC measurements at the specimen shear failure indicate that the magnitude of the transverse compressive strains ε_{22} at the specimen centre could represents 2% of the shear strains γ_{12}. This might look negligible at first, but considering the difference between E_{22} and G_{12}, the stress ratio σ_{22}/τ_{12} is estimated to 10% (assuming no stiffness degradation in shear). If the assumption of pure shear at the specimen gauge section can not be made, a multi-axial failure criterion must be used to derive the shear strength from the stress at failure. In this case, the influence of σ_{22} stresses on the measured shear stress–strain response is not accounted for as their magnitude is still relatively low with respect to τ_{12} stresses. However, the Iosipescu shear test method would benefit

from further research on the prevention of specimen premature splitting failure and reducing the magnitude of parasitic transverse stresses in the region between the notches.

5.2 Uniaxial and biaxial transverse compression tests

As mentioned previously, a direct 2–3 shear loading, using thick UD Iosipescu specimens for instance, only allows the measurement of the elastic shear modulus. The entire shear stress–strain curve cannot be extracted from any of the shear test methods available today, because a premature tensile failure always results in the catastrophic failure of the test specimen. However, it is well accepted that the failure of a UD laminate under transverse compressive stresses is driven by shear.

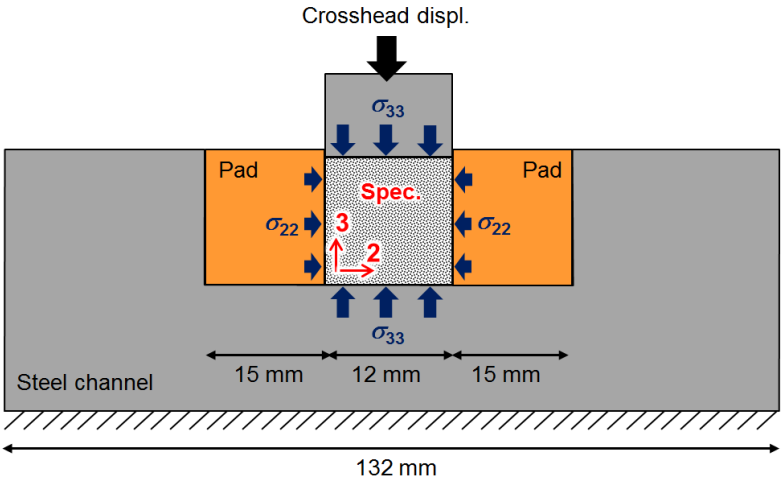

Figure 13: Channel-die test setup for biaxial transverse compression test, from **Paper F**.

In **Paper F**, uniaxial compression and biaxial transverse compression tests are performed on the HTS45/LY556 composite studied in this thesis. Using prismatic (cube) specimens for the uniaxial σ_{33} compression tests led to similar results in terms of stiffness E_{33} and compressive strength Z_c as when using the double waisted specimen design proposed by Ferguson *et al.* [13]. This finding should be verified by investigating different composite material systems, but it could potentially lead to simplified through-thickness compression test methods. For the biaxial σ_{33}–σ_{22} compression tests, prismatic specimens were used again but this time the specimen is placed inside a channel-die rig [64] in order to constrain the 2–direction, as shown in Fig. 13. All the surfaces of the specimen are lubricated in order to reduce friction and therefore reduce the amount of shear stresses in the specimen. The pad material selected, a plain weave glass/polyester composite, is strong enough to not break during the test and its stiffness result in a biaxial stress ratio σ_{22}:σ_{33} of 1:5.3 in the specimen. The transverse shear stress τ_T on the failure plane shown in Fig. 10 is obtained from the stress transformation equation

$$\tau_T = -\frac{\sigma_{22} - \sigma_{33}}{2} \sin(2\alpha), \tag{1}$$

where σ_{33} is obtained from the load cell, σ_{22} is estimated from pad stiffness and the DIC strain readings in the pads, and the inclination of the plane α is determined from the DIC strain readings on the UD specimen. The transverse shear strain γ_T is calculated along the matrix failure plane by rotating the coordinate system of the DIC system with the angle α. In the uniaxial σ_{33} compression tests, the same procedure to extract the transverse shear response is followed with the only difference being that $\sigma_{22} = 0$ in Eq. 1 (no constraint in the 2–direction).

5.3 Calibration of the matrix damage model from the experimental shear responses

The damage model presented in Section 4 requires a set of parameters to be determined from experimental longitudinal and transverse shear responses of UD laminates. In particular, the matrix compression and the longitudinal compression failure modes are shear sensitive and require a careful calibration of the model from experimental shear results.

Fig. 14 shows the entire longitudinal shear and transverse shear responses measured experimentally in **Paper B** and **Paper F** for the HTS45/LY556 uni-weave NCF material investigated in this thesis. The response of the model after calibration is also shown for comparison. In practise the shear responses are used to identify the model parameters, so it is normal that the simulation fits the experimental results. What is not calibrated from the experiments is the pressure dependency of the longitudinal and transverse shear responses. Fig. 14 indicates that the model account for a correct pressure dependency of τ_T for the two transverse compression cases investigated. The model parameters calibrated from the curves in Fig. 14 are reported in Table 4. Once the model parameters are identified, simulation can be used for validation on coupons that have not been used for the calibration procedure (e.g. simulation of the crush coupon and the transverse compression test specimen in **Paper E**).

As mentioned previously, the nonlinear shear behaviour in the model is a result of an increase in the amount of matrix microcracks and the associated frictional effects from the sliding of microcrack surfaces. The damage is also associated with irreversible strains, whose evolution can be monitored experimentally with full unloading at different load levels. Cyclic Iosipescu tests were performed for this purpose and the resulting longitudinal shear stress–strain curve for one specimen is plotted in Fig. 14. The area enclosed inside the hysteresis loops generated during the unloading/reloading cyclic represents the energy dissipated in the damaged material. For the model parameter identification process, the cyclic test data helps for the identification of the pair of parameters (μ_L, p_{0L}). Unfortunately no cyclic test results for transverse shear are available at the moment so the calibration of the model parameters related to transverse shear response relies only on the experimental results of shear specimens loaded in monotonic conditions.

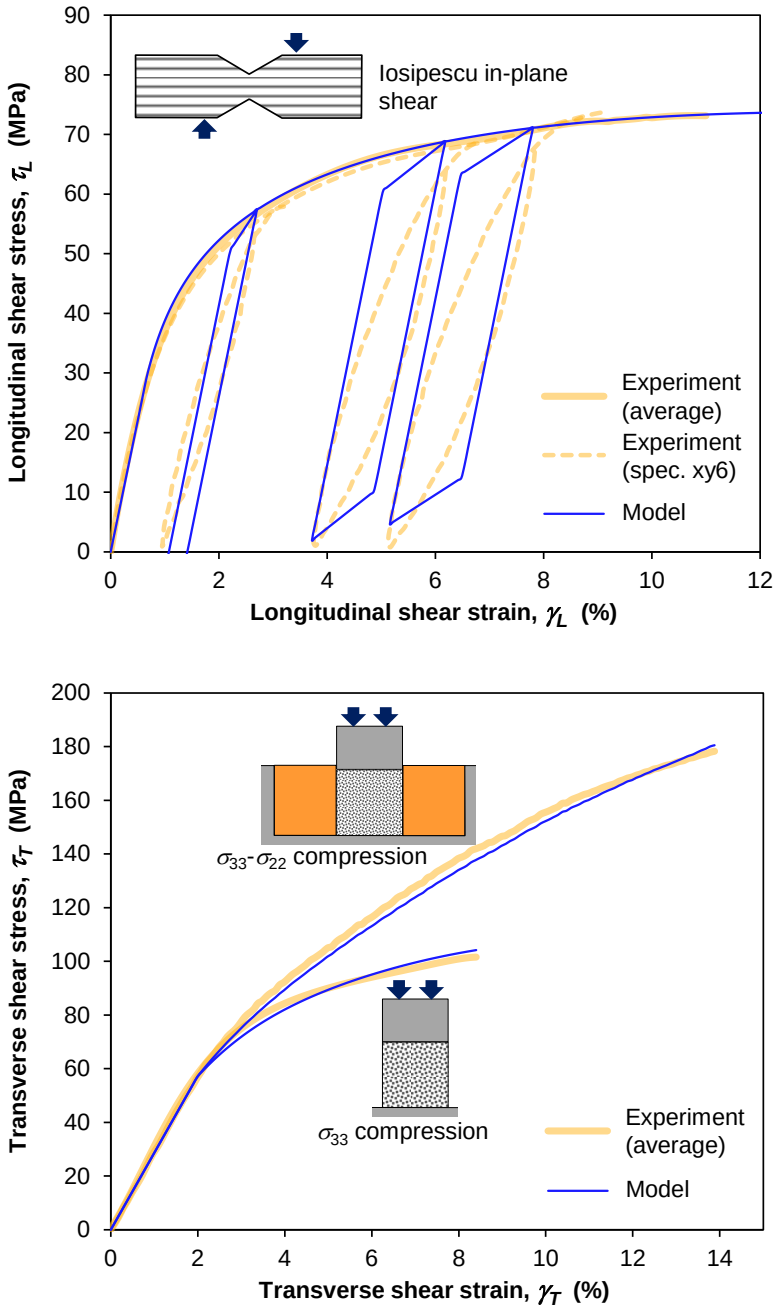

Figure 14: Calibration of the shear part of the ply-based damage model from experiments (longitudinal shear up, transverse shear down).

6 Crush test on flat coupons

6.1 Crushing of UD coupons

Laminated tubes, corrugated plates, or more complex structures have been extensively used to investigate the specific energy absorption of a given material/structure system. Those tests capture the entire complexity of the crushing process, which makes it

Table 4: Model parameters calibration from experimental shear responses.

Model parameter	**Value**
Longitudinal shear	
Stress at damage onset, τ_{0L} (MPa)	23
Friction coefficient, μ_L ()	0.42
Internal pressure, p_{0L} (MPa)	70
Contact stiffness, K_L (MPa)	4500
Transverse shear	
Stress at damage onset, τ_{0T} (MPa)	57
Friction coefficient, μ_T ()	0.35
Internal pressure, p_{0T} (MPa)	30
Common to longitudinal and transverse shear	
Exponent in damage evolution law, p ()	-0.65

difficult to interpret the morphology of the crush front and to use the results for the development of material models for crash. However, those tests are good candidates for the validation procedure of mature numerical codes in a later stage of research (i.e. stage 2 of the building block approach pyramid in Fig. 5).

The crushing of composite plies can be investigated by crushing UD specimens. The failure of standard UD test specimens for uniaxial in-plane compression tests is catastrophic. However, if triggering mechanisms are used stable progressive failure at a constant crush stress can be achieved through the test without catastrophic failure. A trigger generally consists of a geometric feature introduced at one end of a specimen to create a stress concentration and initiate crushing. The most common trigger type is the bevel trigger (illustrated on a crash tube in Fig. 1). It is important to differentiate the crush stress of a ply from the strength of a ply. Referring to the constitutive response of the material model in Fig. 9, the crush stress corresponds to the stress in the plateau region while the peak stress of the curve corresponds to the strength measured from compression tests.

In **Paper C** a simple flat crush coupons geometry is proposed to extract the quasi-static crushing response of unidirectional HTS45/LY556 laminates. The same specimen geometry is used in **Paper D** to investigate the effect of fibre orientation on the crushing behaviour of the laminate, and in **Paper E** for the validation procedure of the matrix compression/shear failure mode of the ply-based model selected for this thesis. The specimen geometry is shown in Fig. 15. An arrow shaped trigger[4] was selected in order to limit the amount of out-of-plane failure by splaying during crushing, as explained later in this section. Although it is far from being a representation structure to be used in a real crash assembly, the flat coupons can be

[4]The arrow shaped trigger is denoted triangular through-thickness (TTT) trigger in **Paper C** and **Paper D**.

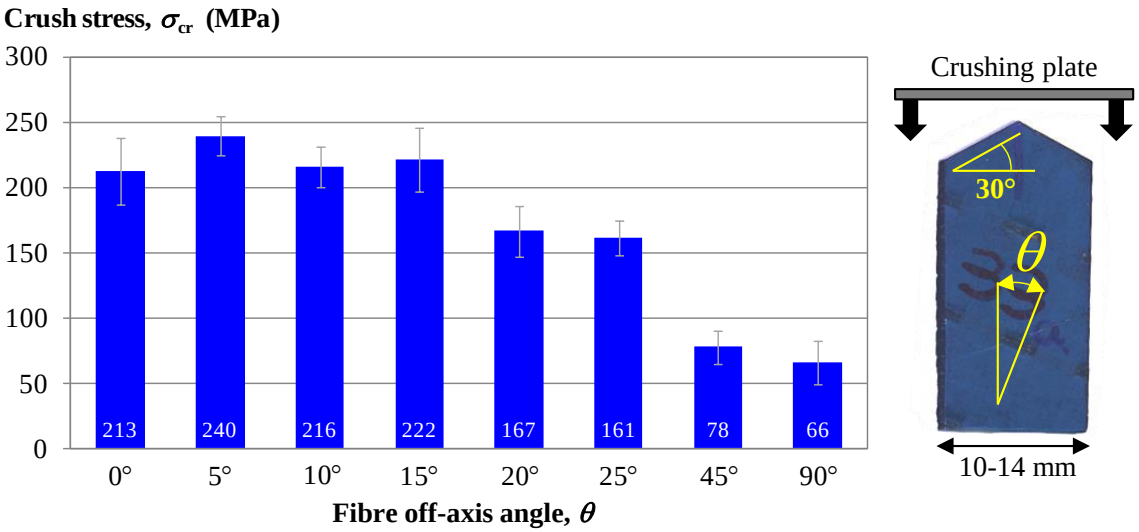

Figure 15: Average crush stress in UD HTS45/LY556 flat coupons with different off-axis angles, from **Paper D**.

used successfully to describe the crushing behaviour of the material and to measure stress levels associated with progressive failure during crushing.

The results of the crush stress evaluation of the HTS45/LY556 uni-weave NCF material as a function of the fibre orientation are shown in Fig. 15. The crush stress is evaluated during crushing of the specimen trigger. Fig. 15 indicates that the crush stress remains relatively unchanged for fibre off-axis angles between 0–15° and then reduces considerably for larger off-axis angles. The failure analysis of the specimens (which consists of observing polished crush zone cross-sections with an optical microscope) revealed that the change in crush stress is associated with a change of failure mode. The main failure mechanism is fibre kinking in the 0–15° specimens and matrix compression/shear in the 45–90° specimens. In 0–15° specimens, the kink-bands are mostly oriented in the through-thickness direction of the laminates. The in-plane shear stresses introduced from the loading of the in-plane fibre off-axis specimens are not expected to have a strong influence on the through-thickness kinking mechanism. This supports the observations on the constant crush stress measured for $0° \leq \theta \leq 15°$.

Although the crush stress is not directly used as an input to the material model selected for this thesis, it is in any case a useful measurement to evaluate the predictive capability of the model. In Gutkin *et al.* [50] the analytical kinking model for fibre compression is validated against the crush stress measured experimentally with the arrow shaped coupons. The results, shown in Fig. 16, indicate that the model predicts a value for the mean crush stress which is in good agreement with the experimental results. The model also predicts that the crush stress is fairly insensitive to fibre misalignment, which is is in agreement with the experimental results in Fig. 15 for small fibre off-axis angles. However, it is clearly visible from Fig. 16 that fibre misalignment is having a large influence on the longitudinal compressive strength.

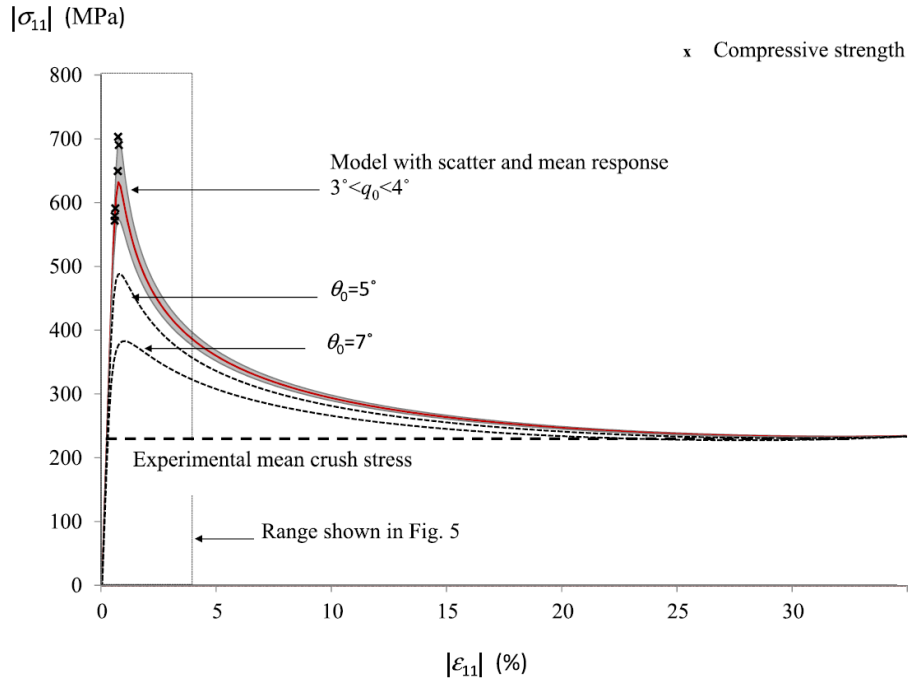

Figure 16: Evolution of kinking stress vs. experimental results for the HTS45/LY556 material system: Strength and mean crushing stress [50].

Thanks to the simple geometry of the flat coupon, it is relatively straightforward to correlate features in the load–displacement curves with physical failure observations. For instance, it was observed in **Paper C** than the arrow shaped trigger led to higher crushing loads than the conventional bevel trigger. The observation of the crush zone morphology indicated a large difference in the amount of fragmentation and splaying failure between the two specimen types. The arrow shaped trigger promotes fracture by fragmentation, which is a more efficient crushing mode than splaying in term of energy absorption and therefore yields higher crush loads. The bevel trigger introduces a large amount of delaminations right from the beginning of the crushing process. This results in a failure mode being largely dominated by splaying and in a crush stress of only half the value measured in specimens with an arrow shaped trigger.

6.2 Crushing of multidirectional coupons and tubes

The arrow shaped crush coupon geometry was also used to investigate the crushing behaviour of multidirectional HTS45/LY556 laminates, although this work is not reported in the appended papers of this thesis. In addition, HTS45/LY556 cross-ply laminated tubes were tested in axial crushing conditions within the project "Modelling crash behaviour in future lightweight composite vehicles – step 1" [42]. The results of these tests will be used in the future for further validation of the damage model being developed in parallel to this research. The challenges associated with crushing of multidirectional laminates are to accurately predict the extent of

delaminations and the complex interactions of intralaminar failure modes.

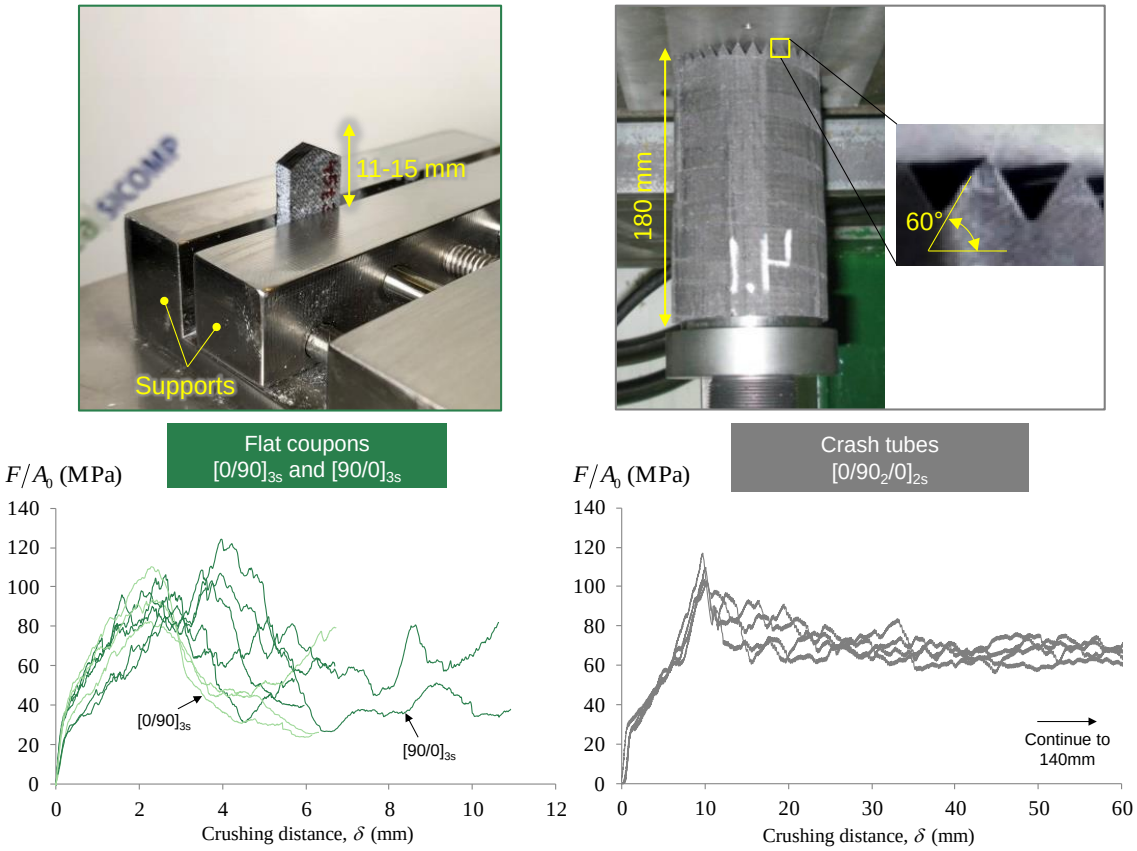

Figure 17: Results of quasi-static crush tests on cross-ply HTS45/LY556 laminates using small flat coupons and using larger crash tube structures.

The size difference between the flat coupons and the crash tubes can clearly be seen in Fig. 17. The available crushing distance in the flat coupons was less than 15 mm while the crash tubes were crushed over a distance of 140 mm. The trigger of the crash tubes resembles the one of the flat coupons although the trigger angle and trigger height are different. The crushing curves of flat coupons and crash tubes, shown in Fig. 17, share some similarities. The values for the peak stress are quite close. The peak stress corresponds to the point at which the trigger is entirely crushed. A sustained crush stress is reached in the tube specimens after the peak stress. In the flat coupons this stable crush stress plateau is less marked. It can be tempting to compare directly the crushing curves of the two specimen types. However, it is well established that even though similar material and lay-ups[5] are used, the stress–displacement curves and the associated specific energy absorption are highly sensitive to the specimen geometry.

The crushing modes of the multidirectional flat coupons and tubes is a mixed-mode of fragmentation and splaying. The images obtained from a travelling microscope pointing at the edge of the flat coupon in Fig. 18 indicate that the laminate is

[5]Here both specimens are cross-ply laminates but the lay-ups are not identical. The laminate thickness also differs between the two specimen types.

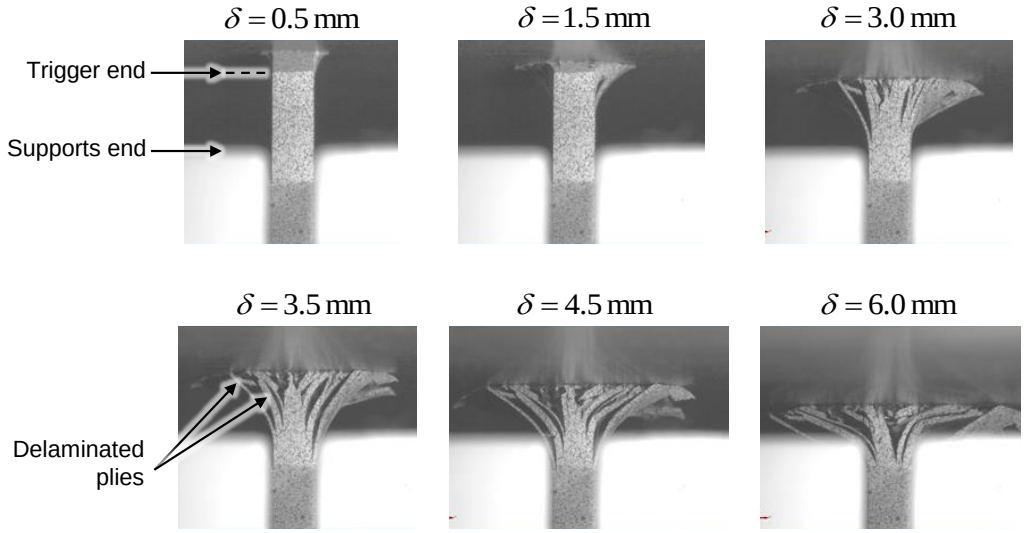

Figure 18: Edge of a $[0/90]_{3s}$ crush coupon observed at different crushing distances δ.

undergoing significant amount of delaminations during crushing. For large crushing distances the delaminations propagate inside the supported region of the specimen. Therefore, if the results are to be correlated numerically the effect of the specimen supports must be considered in the simulations. In the crash tubes, delaminations were observed as deep as 7 mm to 20 mm below the crush front. It was found that the deepest delaminations originated from wrinkled regions in the tubes[6].

6.3 Comparison between model predictions and experiments

Fig. 19 shows the correlation between the crush experiments of UD flat coupons with 45° oriented fibres (c.f. Section 6.1) and FE results obtained with ABAQUS/Explicit 2016. The ABAQUS simulations were run using the matrix compression/shear ply-based material model combining damage and friction which is described in Section 4. As mentioned previously, the model input parameters are determined from material characterisation tests on HTS45/LY556 composites, including the damage evolution law and friction properties identification from cyclic Iosipescu shear tests. In the arrow shaped coupons with 45° fibres the main failure mechanism is fragmentation of the laminates by matrix compression and shear failure. Because this failure mode is isolated from the other intralaminar failure modes, the experimental results can be used directly to validate the MC (matrix compression/shear) part of the damage model. Fig. 19 shows a good agreement between the experiments and the simulations. The simulations are relatively insensitive to delaminations, which supports the physical observation (from post-mortem specimen failure investigation) that the crushing process is not involving delamination.

In **Paper E** an additional validation is reported for an arrow shaped crush coupon

[6]Wrinkles are imperfections introduced during the lamination of the tubes.

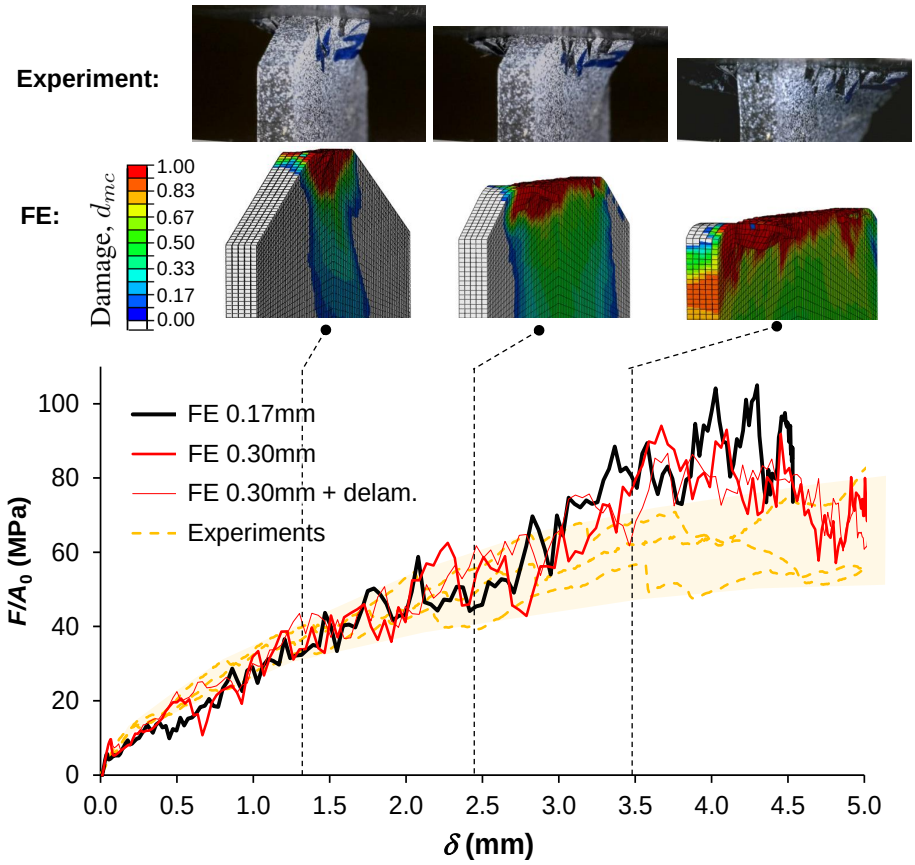

Figure 19: Experimental and numerical crushing response of the $[45°]_{10}$ arrow shaped coupons, from **Paper E**.

with fibres oriented in the transverse direction to the crushing direction. Similarly to the crushing of 45° off-axis coupons, the progressive failure mode is driven by matrix shear and compressive failure.

Regarding the crushing behaviour of UD flat coupons in which fibre failure is the main damage mechanism, i.e. 0–25° specimens in Fig. 15, the current FE implementation of the kinking model developed in [49, 50] is not robust enough to allow for stable FE simulation of the flat coupons. As a first step, a validation of the analytic kinking model using the crush stress measured experimentally is available in [50].

To assess the predictive capability of FE simulations of multidirectional crush specimens, it is necessary that the ply-based material model accounts for all intralaminar failure modes and interact with an interlaminar damage model to capture delaminations. Delaminations have been found to play a major role in the amount of fragmentation and splaying of multidirectional crush specimens. Therefore, delamination growth must be modelled accurately in order to capture the correct progressive fracture processes of a crush coupon or structure. The nature and extent of damage in the continuous fronds formed during splaying are influenced by the degree of curvature the fronds experienced, which itself is influenced by the position

and the depth of delaminations ahead of the crush front. At this stage of research, no numerical simulations have yet been performed on multidirectional flat coupons and crash tubes (the experimental results are reported in Section 6.2).

7 Summary of the appended papers

In **Paper A** an extensive mechanical characterisation of the uni-weave carbon/epoxy NCF reinforced composite (HTS45/LY556) investigated in this thesis is performed. The ply properties are characterised in terms of elastic moduli, strengths, and failure characteristics for different loading directions. This includes the through-thickness direction since the material investigated is orthotropic. The weft threads of the NCF reinforcement are responsible for a reduction of 50% in strength for through-thickness tension tests compared to in-plane transverse tension tests. They initiate an interlaminar failure in the through-thickness tests, which results in a relatively low strength. Similarly, the weft threads are responsible for a premature interlaminar failure in the 1–3 Iosipescu shear specimens. Finally, the mechanical properties database of the material is completed with interlaminar and intralaminar (only for the fibre failure modes) fracture toughness properties. Rarely have the mechanical and fracture properties of a composite material system been evaluated so thoroughly and shared with the scientific community. The lack of access to material data acts as a hindrance to research. It is not uncommon that researchers and engineers are assuming material data in their analytical or FE models because the required input are not available in the literature. By publishing **Paper A** in an open access journal, the article can reach a larger potential audience and provide guidelines for the characterisation of composites to many industries.

Paper B focuses on Iosipescu shear experiments. The shear response is the foundation for the development of the damage model supported in this work. Knowing the difficulty associated with shear testing of composites, the quality of the Iosipescu shear test for the material investigated in this work is assessed experimentally with full-field DIC strain measurements and numerically with an FE analysis of the test specimen in the first part of the paper. The results indicate that a fairly uniform and pure shear stress state is achieved in the specimen gauge section, which is a requirement for an accurate evaluation of the material shear behaviour. Premature failure by splitting at the notches is inevitable with the current specimen design. However, the DIC and FE results indicate that this failure mode is not detrimental to the quality of the data produced during the test. In the second part of the paper, the experimental cyclic 1–2 and 1–3 shear stress–strain curves are used to calibrate two ply-based CDM material models for CFRP materials. The data extracted from the cyclic shear curves are the damage evolution law and the plasticity parameters for the model by Ladevèze & Le Dantec [65], and the damage evolution law and the friction parameters for the model by Gutkin & Pinho [48]. The material model coupling damage and friction [48] is further developed in **Paper E**. The two models can accurately predict the nonlinear monotonic shear stress–strain curve and the

accumulation of permanent shear strains. However, only the material model coupling damage and friction is able to capture (to some extent) the hysteresis loops generated during unloading/reloading of the material.

The contribution of **Paper C** is concerned with the development of a simple test method to measure the longitudinal and the transverse crush stress of composite plies. With an appropriate choice of trigger, the progressive failure of a UD flat coupon of small dimensions is associated with a stable crush stress. For longitudinal crushing, the traditional bevel trigger leads to out-of-plane specimen failure by splaying with a limited amount of in-plane fracture. In contrast, the proposed arrow shaped trigger achieves a high amount of compressive fragmentation failure. The longitudinal crush stress associated with the splaying-dominated failure mode is roughly half the crush stress associated with the fragmentation-dominated failure mode. This highlights the importance of maximising the amount of 0° plies fragmentation in energy absorbing components. For transverse crushing, the crushing mode is by fragmentation for the two trigger types investigated. After testing, a failure investigation is carried out to identify the different damage mechanisms in the specimens.

Paper D follows up the work in **Paper C** and focuses on the crushing response of off-axis UD laminates (fibre off-axis angles of 5°, 10°, 15°, 20°, 25° and 45°). The crush stress for each off-axis angle is evaluated from the load–displacement curve and the failure mode of the specimen is discussed from the observation of the crush zone morphology with an optical microscope. An important finding of this study is that for small in-plane fibre off-axis angles (up to 15°) the crush stress remains unchanged and the dominant failure mechanism is through-thickness fibre kinking in all cases. The experimental results can be used for the validation of progressive damage models for fibre compressive failure modes and for matrix compression/shear failure modes. The test can also be used as a simple method for quantifying and ranking the crush behaviour of different composite materials.

In **Paper E** an orthotropic ply-based material model for crushing of composites is developed and validated against experiments. The material model includes all intralaminar failure modes relevant in CFRP crash scenarios, although the focus of the paper is on the matrix compression/shear failure mode. The CDM material model follows a fixed crack plane approach, i.e. the constitutive material response is evaluated on the fracture plane where damage is originally initiated. In the model formulation damage is coupled with friction to account for the energy dissipated from the sliding of crack surfaces. The constitutive material response on the fracture plane for the matrix compression/shear damage model is obtained from data extracted from in-plane shear experiments and does not require the measurement of the fracture toughness. The validation procedure of the model includes a through-thickness compression specimen (from **Paper A**) and the quasi-static crushing of a UD arrow shaped coupon with fibres oriented either at 45° or 90° to the crushing direction (from **Paper C** and **Paper D**, respectively). A comparison between the experimental and the numerical results confirms the predictive capability of the developed FE tool.

Paper F is concerned with the transverse shear evaluation of the HTS45/LY556 material investigated in this thesis. The material model developed in **Paper E**

requires the entire longitudinal and transverse shear response of the material to be known. While the longitudinal shear behaviour can be evaluated with Iosipescu shear tests, it is not possible to achieve a valid shear failure with any 2–3 shear test available today. However, considering that the failure of a UD specimen under transverse compression occurs by shear in an inclined matrix failure plane, it is theoretically possible to extract a material shear response from an external transverse compressive stress state. The methodology to follow is described in the paper. It uses stress transformation equations and local strain measurements to extract the transverse shear stress–strain response on the failure plane. The specimens are tested under uniaxial transverse compression and biaxial transverse compression to investigate the pressure dependency of the shear response. A channel-die setup is used for the biaxial tests. The specimen is tested in through-thickness compression while constrained in the 2–direction. The main advantage of this setup is that is does not require a biaxial testing machine (only a few laboratories are equipped with a biaxial testing machine).

8 Future work

The previous discussion has demonstrated that crushing of composite structures is an extremely complex process that needs to be broken down into simpler parts in order to develop reliable physically based models. The confidence in the models must be gained through validation of simulations against well designed experiments and through an accurate material characterisation from which the required model parameters are determined.

A considerable amount of the energy absorption during crushing is dissipated by friction. The general approach in FE simulations to account for the friction forces generated between delaminated surfaces and between the composite structure and the impactor is to use contact algorithms. The measurements of friction coefficients, which are input parameters to the contact algorithms, are often omitted from crashworthiness simulation studies although standard tests methods available for plastic sheets can also be applied to composites [66]. The friction properties for composite/composite interfaces and composite/metal interfaces will be investigated in the future to complete the material database on the HTS45/LY556 composite.

Crash events are by definition dynamic events, so strain rate effects —on the material stress–strain curves and on the friction properties— must be evaluated experimentally and included in FE codes, although this is out of the scope of this research. Experimental methods for material characterisation of composites at intermediate and high strain rates are relatively new, time consuming, and require expert staff to interpret the results. Some properties, e.g. interlaminar fracture toughness, can currently still not be measured accurately over a wide range of strain rates. The development of dynamic testing methods is an important aspect for modelling composite crashworthiness and require future research.

Another research task concerns the further development of the biaxial test method introduced in **Paper F**. In order to build a complete biaxial failure envelope several biaxial stress ratios must be evaluated. The degree of lateral constraint in the specimen could be changed by varying the stiffness of the pad material, or by using springs instead of pads in the test setup.

Finally, in order to enhance the energy absorption capabilities of composite crash structures it is necessary to identify the material properties and the fracture processes that encourage high energy absorption mechanisms. New composite materials designed for high energy absorption can then developed based on the physical observations. The architecture of these materials may differ significantly from those of conventional prepeg or NCF materials (e.g. 3D-woven composites [67] or tufted composites [68]). Specific material characterisation methods and progressive damage models must be developed for these materials.

9 References

1. *European Commission* [Accessed online; 30 July 2018]. https://ec.europa.eu/clima/policies/transport/vehicles_en.
2. Fontaras, G., Zacharof, N.-G. & Ciuffo, B. Fuel consumption and CO2 emissions from passenger cars in Europe – Laboratory versus real-world emissions. *Progress in Energy and Combustion Science* **60,** 97–131 (2017).
3. *Special report: Can carbon fibre compete in mainstream automotive?* (Automotive World Ltd, Pernarth, 2018). https://www.automotiveworld.com/research/special-report-can-carbon-fibre-compete-mainstream-automotive/.
4. *First Light – The story behind the McLaren MP4/1* [Accessed online; 31 July 2018]. https://mylifeatspeed.com/first-light-the-story-behind-the-mclaren-mp41/.
5. *Carbon footprint* (Crash Test Technology International, September 2012, 36–40).
6. *Euro NCAP* [Accessed online; 7 August 2018]. https://www.euroncap.com/.
7. Brecher, A. *A safety roadmap for future plastics and composites intensive vehicles* tech. rep. DOT HS 810 863 (U.S. Department of Transportation, 2007).
8. Jiménez, M. A., Miravete, A., Larrodé, E. & Revuelta, D. Effect of trigger geometry on energy absorption in composite profiles. *Composite Structures* **48,** 107–111 (2000).
9. Mamalis, A. G., Manolakos, D. E., Demosthenous, G. A. & Ioannidis, M. B. *Crashworthiness of Composite Thin-Walled Structures* (CRC Press, 1998).
10. Hull, D. A unified approach to progressive crushing of fibre-reinforced composite tubes. *Composites Science and Technology* **40,** 377–421 (1991).
11. Tan, W. & Falzon, B. G. Modelling the crush behaviour of thermoplastic composites. *Composites Science and Technology* **134,** 57–71 (2016).
12. ASTM D3039 / D3039M-08. *Standard test method for tensile properties of polymer matrix composite materials* (ASTM International, West Conshohocken, PA, 2008).
13. Ferguson, R. F., Hinton, M. J. & Hiley, M. J. Determining the through-thickness properties of FRP materials. *Composites Science and Technology* **58,** 1411–1420 (1998).
14. ASTM D3410 / D3410M-03. *Standard test method for compressive properties of polymer matrix composite materials with unsupported gage section by shear loading* (ASTM International, West Conshohocken, PA, 2008).
15. ASTM D6641 / D6641M-16e. *Standard test method for compressive properties of polymer matrix composite materials using a Combined Loading Compression (CLC) test fixture* (ASTM International, West Conshohocken, PA, 2016).

16. ASTM D5448 / D5448M-16. *Standard test method for inplane shear properties of hoop wound polymer matrix composite cylinders* (ASTM International, West Conshohocken, PA, 2016).

17. ASTM D3518 / D3518M-13. *Standard test method for in-plane shear response of polymer matrix composite materials by tensile test of a ±45° laminate* (ASTM International, West Conshohocken, PA, 2013).

18. ASTM D5379 / D5379M-05. *Standard test method for shear properties of composite materials by the V-notched beam method* (ASTM International, West Conshohocken, PA, 2007).

19. ASTM D7078 / D7078M-12. *Standard test method for shear properties of composite materials by V-notched rail shear method* (ASTM International, West Conshohocken, PA, 2012).

20. ASTM D2344 / D2344M-16. *Standard test method for short-beam strength of polymer matrix composite materials and their laminates* (ASTM International, West Conshohocken, PA, 2016).

21. Neumeister, J. & Pålsson, A. Inclined double notch shear test for improved interlaminar shear strength measurements. *Journal of Composites, Technology and Research* **20,** 100–107 (1998).

22. ASTM D5528 / D5528M-01. *Standard test method for mode I interlaminar fracture toughness of unidirectional fiber-reinforced polymer matrix composites* (ASTM International, West Conshohocken, PA, 2017).

23. ASTM D7905 / D7905M-14. *Standard test method for determination of the mode II interlaminar fracture toughness of unidirectional fiber-reinforced polymer matrix composites* (ASTM International, West Conshohocken, PA, 2014).

24. ASTM D6671 / D6671M-13e1. *Standard test method for mixed mode I-mode II interlaminar fracture toughness of unidirectional fiber reinforced polymer matrix composites* (ASTM International, West Conshohocken, PA, 2013).

25. Pinho, S. T., Robinson, P. & Iannucci, L. Fracture toughness of the tensile and compressive fibre failure modes in laminated composites. *Composites Science and Technology* **66,** 2069–2079 (2006).

26. Catalanotti, G., Arteiro, A., Hayati, M. & Camanho, P. Determination of the mode I crack resistance curve of polymer composites using the size-effect law. *Engineering Fracture Mechanics* **118,** 49–65 (2014).

27. Brunner, A., Blackman, B. & Davies, P. A status report on delamination resistance testing of polymer–matrix composites. *Engineering Fracture Mechanics* **75.** Fracture of Composite Materials, 2779–2794 (2008).

28. Koerber, H., Xavier, J. & Camanho, P. High strain rate characterisation of unidirectional carbon-epoxy IM7-8552 in transverse compression and in-plane shear using digital image correlation. *Mechanics of Materials* **42,** 1004–1019 (2010).

29. Ploeckl, M., Kuhn, P., Grosser, J., Wolfahrt, M. & Koerber, H. A dynamic test methodology for analyzing the strain-rate effect on the longitudinal compressive behavior of fiber-reinforced composites. *Composite Structures* **180,** 429–438 (2017).

30. Kuhn, P., Catalanotti, G., Xavier, J., Camanho, P. & Koerber, H. Fracture toughness and crack resistance curves for fiber compressive failure mode in polymer composites under high rate loading. *Composite Structures* **182,** 164–175. ISSN: 0263-8223 (2017).

31. Kuhn, P., Catalanotti, G., Xavier, J., Ploeckl, M. & Koerber, H. Determination of the crack resistance curve for intralaminar fiber tensile failure mode in polymer composites under high rate loading. *Composite Structures* **204,** 276–287 (2018).

32. Jacob, G. C., Fellers, J. F., Simunovic, S. & Starbuck, J. M. Energy absorption in polymer composites for automotive crashworthiness. *Journal of Composite Materials* **36,** 813–850 (2002).

33. *CZone for Abaqus* [Accessed online; 3 August 2018]. `https://www.3ds.com/products-services/simulia/products/abaqus/add-ons/czone/`.

34. McGregor, C., Zobeiry, N., Vaziri, R., Poursartip, A. & Xiao, X. Calibration and validation of a continuum damage mechanics model in aid of axial crush simulation of braided composite tubes. *Composites Part A: Applied Science and Manufacturing* **95,** 208–219 (2017).

35. *LS-Dyna Keyword User Manual – Volume II. Material Models.* tech. rep. Version R10.0 (Livermore Software Technology Corporation, Livermore, USA, 2017).

36. Pinho, S. T., Carlos, D. G., Camanho, P. P., Iannuci, L. & Robinson, P. *Failure models and criteria for FRP under in-plane or three-dimensional stress states including shear nonlinearity* tech. rep. NASA/TM-2005-213530 (NASA Langley Research Center, Hampton, 2005).

37. Andersson, M. & Petter, L. *Crash behaviour of composite structures–A CAE benchmarking study.* Master's thesis, Chalmers University of Technology, Gothenburg, Sweden (2014).

38. Cherniaev, A., Butcher, C. & Montesano, J. Predicting the axial crush response of CFRP tubes using three damage-based constitutive models. *Thin-Walled Structures* **129,** 349–364 (2018).

39. Feraboli, P., Wade, B., Deleo, F., Rassaian, M., Higgins, M. & Byar, A. LS-DYNA MAT54 modeling of the axial crushing of a composite tape sinusoidal specimen. *Composites Part A: Applied Science and Manufacturing* **42,** 1809–1825 (2011).

40. Rouchon, J. Certification of large airplane composite structures, recent progress and new trends in compliance philosophy. *ICAS* **2,** 1439–1447 (1990).

41. Presentation by Johan Jergeus from Volvo Cars (Workshop on crash behaviour of composites, Chalmers University of Technology, Gothenburg, Sweden, 13-14 September 2018).

42. *Modellering av krockbeteendet i framtida lättviktsfordon – steg 1/2 (Modelling crash behaviour in future lightweight composite vehicles – step 1/2)* VINNOVA, Dnr: 2012-03673 and 2016-04239.

43. *Tillförlitlig krockmodellering av fiberkompositer för lättviktsfordon – compcrash2 (Reliable crash modelling of fibre composites for lightweight vehicles – compcrash2)* Swedish Energy Agency, Dnr: 34181-2.

44. Främby, J. *On efficient modelling of progressive damage in composite laminates using an equivalent single-layer approach* Licenciate thesis, Chalmers University of Technology, Göteborg, Sweden (2016).

45. *Porcher Industries. Selector guide composites* [Accessed online; 10 August 2018]. `https://www.porcher-ind.com/upload/media_center/dab29-selector-guide-composites.pdf`.

46. *Huntsman. Selector guide for composite resin systems* [Accessed online; 10 August 2018]. `http://www.huntsman.com/advanced_materials/Media%5C%20Library/global/files/EUR_Composites%5C%20-%5C%20Composite%5C%20Resin_Araldite_Epoxy_RTM.pdf`.

47. Wilhelmsson, D., Gutkin, R., Edgren, F. & Asp, L. An experimental study of fibre waviness and its effects on compressive properties of unidirectional NCF composites. *Composites Part A: Applied Science and Manufacturing* **107,** 665–674 (2018).

48. Gutkin, R. & Pinho, S. T. Combining damage and friction to model compressive damage growth in fibre-reinforced composites. *Journal of Composite Materials* **49,** 2483–2495 (2015).

49. Costa, S., Gutkin, R. & Olsson, R. Mesh objective implementation of a fibre kinking model for damage growth with friction. *Composite Structures* **168,** 384–391 (2017).

50. Gutkin, R., Costa, S. & Olsson, R. A physically based model for kink-band growth and longitudinal crushing of composites under 3D stress states accounting for friction. *Composites Science and Technology* **135,** 39–45 (2016).

51. González, C. & LLorca, J. Mechanical behavior of unidirectional fiber-reinforced polymers under transverse compression: Microscopic mechanisms and modeling. *Composites Science and Technology* **67,** 2795–2806 (2007).

52. Melin, L. G., Neumeister, J., Pettersson, K. B., Johansson, H. & Asp, L. E. Evaluation of four composite shear test methods by digital speckle strain mapping and fractographic analysis. *Journal of Composites Technology & Research* **22,** 161–172 (2000).

53. Gutkin, R., Pinho, S., Robinson, P. & Curtis, P. On the transition from shear-driven fibre compressive failure to fibre kinking in notched CFRP laminates under longitudinal compression. *Composites Science and Technology* **70,** 1223–1231 (2010).

54. Puck, A. & Schürmann, H. Failure analysis of FRP laminates by means of physically based phenomenological models. *Composites Science and Technology* **58,** 1045–1067 (1998).

55. Kumosa, M., Odegard, G., Armentrout, D., Kumosa, L., Searles, K. & Sutter, J. Comparison of the ±45° tensile and Iosipescu shear tests for woven fabric composite materials. **24,** 3–16 (2002).

56. Stojcevski, F., Hilditch, T. & Henderson, L. C. A modern account of Iosipescu testing. *Composites Part A: Applied Science and Manufacturing* **107,** 545–554 (2018).

57. Adams, D. F. & Lewis, E. Q. Experimental assessment of four composite material shear test methods. *Journal of Testing and Evaluation* **25,** 174–181 (1997).

58. Jia, L., Yu, L., Zhang, K., Li, M., Jia, Y., Blackman, B. R. K. & Dear, J. P. Combined modelling and experimental studies of failure in thick laminates under out-of-plane shear. *Composites Part B: Engineering* **105,** 8–22 (2016).

59. Adams, D. F. & Walrath, D. E. Current status of the Iosipescu shear test method. *Journal of Composite Materials* **21,** 494–507 (1987).

60. Bru, T. *Literature survey of the Iosipescu shear test* tech. rep. TR14-009 OPEN (Swerea SICOMP, Mölndal, Sweden, 2014).

61. Walrath, D. E. & Adams, D. F. *Verification and application of the Iosipescu shear test method* tech. rep. UWME-DR-401-103-1 (Department of mechanical engineering, University of Wyoming, Laramie, Wyoming, USA, 1984).

62. Neumeister, J. M. & Melin, L. N. *A modified Iosipescu shear test for anisotropic composite panels* in *Proceedings of 14th International Conference on Composite Materials (ICCM14)* (San Diego, CA, 14-15 July 2003), 121–129.

63. Melin, N. *The modified Iosipescu shear test for orthotropic materials.* PhD thesis, KTH Royal Institute of Technology, Stockholm, Sweden (2008).

64. Collings, T. A. Transverse compressive behaviour of unidirectional carbon fibre reinforced plastics. *Composites* **5,** 108–116 (1974).

65. Ladevèze, P. & Le Dantec, E. Damage modelling of the elementary ply for laminated composites. *Composites Science and Technology* **43,** 257–267 (1992).

66. ASTM D1894-14. *Standard test method for static and kinetic coefficients of friction of plastic film and sheeting* (ASTM International, West Conshohocken, PA, 2014).

67. Oddy, C., Ekermann, T., Ekh, M., Fagerström, M. & Hallström, S. *Evaluation of damage initiation models for 3D-woven fibre composites* in *Proceedings of the 18th European Conference on Composite Materials ECCM-18* (Athens, Greece, 24-28 June 2018).

68. Blok, L., Kratz, J., Lukaszewicz, D., Hesse, S., Ward, C. & Kassapoglou, C. Improvement of the in-plane crushing response of CFRP sandwich panels by through-thickness reinforcements. *Composite Structures* **161,** 15–22 (2017).